



Universidad Autónoma de San Luis Potosí

Facultad de Ciencias Químicas

Posgrado en Ciencias Farmacobiológicas

“Evaluación farmacodinámica antimicrobiana de
derivados sintéticos de fluoroquinolonas en
bacterias patógenas”

Tesis de grado:

Doctor en Ciencias Farmacobiológicas

Presenta

M en C. Medellín Luna Mitzzy Fátima

Agosto 2023

Acreditación

Proyecto realizado en colaboración de las siguientes instituciones:



Laboratorio de Investigación en
**Inmunotoxicología
y Terapéutica
Experimental**



CENTRO DE INVESTIGACIÓN EN
**CIENCIAS DE LA SALUD
Y BIOMEDICINA**

Laboratorio de Síntesis Orgánica y Laboratorio de Inmunotoxicología y Terapéutica Experimental de la Unidad Académica de Ciencias Químicas de la Universidad Autónoma de Zacatecas

Centro de Investigación en Ciencias de la Salud y Biomedicina de la Universidad Autónomas de San Luis Potosí

Unidad de Investigación en Biomédica IMSS Zacatecas.



El programa de Doctorado en Ciencias Farmacobiológicas de la Universidad Autónoma de San Luis Potosí pertenece al Sistema Nacional de Posgrados (SNP) del CONAHCyT, registro 003384, en el Nivel 291236

Número de registro de beca otorgada por CONCyT/CVU: 778440



Evaluación farmacodinámica antimicrobiana de derivados sintéticos de fluoroquinolonas en bacterias patógenas by Mitzzy Fátima Medellín Luna is licensed under a [Creative Commons Reconocimiento-NoComercial-SinObraDerivada 4.0 Internacional License](https://creativecommons.org/licenses/by-nc-nd/4.0/).

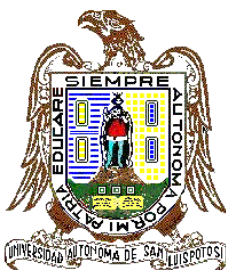
Reporte de similitud

Análisis de la relación estructura actividad de análogos de fluoroquinolonas y la evaluación antimicrobiana del 7-benzimidazol-1-il-fluoroquinolona: en modelos in vitro, in silico e in vivo

INFORME DE ORIGINALIDAD

14%

ÍNDICE DE SIMILITUD



UNIVERSIDAD AUTÓNOMA DE SAN LUIS POTOSÍ

FACULTAD DE CIENCIAS QUÍMICAS

POSGRADO EN CIENCIAS FARMACOBIOLOGICAS

EVALUACIÓN FARMACODINÁMICA ANTIMICROBIANA DE DERIVADOS SINTÉTICOS DE FLUOROQUINOLONAS EN BACTERIAS PATÓGENAS

TESIS PARA OBTENER EL GRADO DE:
DOCTORADO EN CIENCIAS FARMACOBIOLOGICAS

PRESENTA

M EN C. MEDELLÍN LUNA MITZZY FÁTIMA

ASESOR

DRA. DIANA PATRICIA PORTALES PÉREZ

COASESOR

DR. ALBERTO RAFAEL CERVANTES VILLAGRANA

SINODALES

DR. HIRAM HERNÁNDEZ LÓPEZ _____

DR. JULIO ENRIQUE CASTAÑEDA DELGADO _____

DR. FIDEL MARTÍNEZ GUTIÉRREZ _____

DRA. EDGAR LARA RAMÍREZ _____



SAN LUIS POTOSÍ, S.L.P., AGOSTO 2023

Integrantes del Jurado

Los integrantes del jurado están conformados por:

Dra. Diana Patricia Portales Pérez
Directora de tesis
Facultad de Ciencias Químicas, UASLP

Dr. Alberto Rafael Cervantes Villagrana
Co-director de tesis
Unidad Académica de Ciencias Químicas, UAZ

Dr. Hiram Hernández López
Asesor externo
Unidad Académica de Ciencias Químicas, UAZ

Dr. Fidel Martínez Gutiérrez
Asesor Interno
Facultad de Ciencias Químicas, UASLP

Dr. Julio Enrique Castañeda Delgado
Asesor externo
Unidad de Investigación Biomédica, IMSS

Dr. Edgar Lara Ramírez
Asesor externo
Unidad de Investigación Biomédica, IMSS

Este trabajo se lo dedico a mi familia que en todo momento me inspiró, me apoyó y me alentó a no renunciar y seguir adelante sin importar la circunstancia. Y a mi abuelo que sé que está orgulloso porque nunca me rendí.

Agradecimientos

Agradezco al programa de Doctorado en Ciencias Farmacobiológicas de la Facultad de Ciencias Químicas de la Universidad Autónoma de San Luis Potosí por ser la institución que fomento y apoyo mi formación y desarrollo académico.

Agradezco a los laboratorios de Antimicrobianos, Biopelículas y Microbiota del Centro de Investigación en Ciencias de la Salud y Biomédica de la Universidad Autónoma de San Luis Potosí. Al Laboratorio de Síntesis Orgánica, Laboratorio de Inmunotoxicidad y Terapéutica experimental, al Laboratorio de Microbiología y al Bioterio de “Claude Bernard” de la Universidad Autónoma de Zacatecas. Y a la Unidad de Investigación de Ciencias Biomédicas, por el apoyo y la oportunidad de realizar estancias que generaron los experimentos y resultados del presente trabajo de tesis, así como el aprendizaje de diferentes técnicas y formas de trabajo en el laboratorio.

Le agradezco al Dr. Alberto Cervantes, al Dr. Hiram Hernández, al Dr. Julio Castañeda y al Dr. Edgar Lara por ser guía y maestros durante la realización del proyecto de investigación. Además de darme aliento para continuar y culminar a pesar de todos los obstáculos que se presentaron y siempre buscar una solución alternativa.

Le agradezco al Dr. Fidel Martínez Gutiérrez por su valiosa colaboración en la realización de experimentos y en su valiosa participación en mi formación como investigadora. También a la Dra. Diana Portales Pérez, por su guía y apoyo en la realización del proyecto.

Le agradezco a mi madre Rosa Hilda Luna, mi padre José Manuel Medellín y mi hermano José Manuel Medellín Luna por su valiosa participación indirecta en cada paso de la realización del proyecto, su infinita paciencia y tolerancia en aquellos días malos y su amor para comprender y permitirme cumplir mis sueños y metas.

Le agradezco a Néstor Alejandro Camarillo por ser mi amigo, mi colega, mi compañero, chofer, chef, crítico y mi esposo, por brindarme su apoyo incondicional para iniciar y terminar este proyecto de investigación, así como para alcanzar a cumplir mis metas profesionales.

A mis abuelos María del Rosario González y José Manuel Medellín Gutiérrez por ser inspiración para seguir estudiando y no dejarme de preparar, además de ser sustento en los días de frustración y apoyo de paciencia para no rendirme y llegar hasta el final.

Certificado



molecules
an Open Access Journal by MDPI



CERTIFICATE OF ACCEPTANCE

Certificate of acceptance for the manuscript (**molecules-2531806**) titled:
Fluoroquinolone analogues SAR Analysis and the antimicrobial evaluation of 7-benzimidazol-1-yl-
fluoroquinolone in in vitro, in silico, and in vivo models

Authored by:
Mitzy Fátima Medellín-Luna; Hiram Hernández-López; Julio Enrique Castañeda-Delgado; Fidel Martínez-
Gutiérrez; Edgar Lara-Ramírez; Joan Jair Espinoza-Rodríguez;
Salvador García-Cruz; Diana Patricia Portales-Pérez; Alberto Rafael Cervantes-Villagrana

has been accepted in *Molecules* (ISSN 1420-3049) on 07 August 2023



Academic Open Access Publishing
since 1996

Basel, August 2023

Análisis de estructura actividad de análogos de fluoroquinolonas y la evaluación antimicrobiana del 7-benzimidazol-1-il-fluoroquinolona en modelos *in vitro in silico* e *in vivo*

Resumen

Los estudios de Relación Estructura Actividad (REA) permiten evaluar la relación entre los cambios químicos estructurales y la actividad biológica. Las fluoroquinolonas tienen características químicas que permiten modificar su estructura y generar nuevos análogos con propiedades terapéuticas diferentes. El objetivo de esta investigación es identificar y seleccionar el análogo de fluoroquinolona con heterociclo en posición C-7 **FQH 1-5** con actividad antimicrobiana igual o mejor a la fluoroquinolona de referencia por medio de evaluaciones *in vitro*, *in silico* e *in vivo*. Primero se realizó un análisis REA a los **FQH 1-5**, mediante un modelo *in vitro* de sensibilidad antimicrobiana, para seleccionar el mejor compuesto. Posteriormente, el análisis del mecanismo de acción en el modelo *in silico* por acoplamiento molecular. Aunado a ello se evaluó la citotoxicidad en células no bacterianas (células mononucleares de sangre periférica: PBMC's). Y finalmente, se determinó el potencial antimicrobiano por medio de un modelo *in vivo* de infección tópica en ratones. Los resultados demostraron diferencias antimicrobianas entre los **FQH 1-5** y las bacterias Gram positivas y Gram negativas, se identificó al 7-benzimidazol fluoroquinolona (**FQH-2**) como el mejor por su acción antimicrobiana sobre *S. aureus*. Se sugiere que el FQH-2 tiene el mismo mecanismo de acción que las fluoroquinolonas; no se encontraron efectos citotóxicos sobre células no bacterianas (PBMC's); además este compuesto demostró disminuir la cantidad de bacterias en el tejido de la herida infectada.

Palabras clave: Relación estructura actividad, Análogo de fluoroquinolona, antimicrobiano, *S. aureus*

Fluoroquinolone analogues SAR Analysis and the antimicrobial evaluation of 7-benzimidazol-1-yl-fluoroquinolone in *in vitro*, *in silico*, and *in vivo* models

Abstract

Structure Activity Relationship (SAR) studies allow the evaluation of the relationship between structural chemical changes and biological activity. Fluoroquinolones have chemical characteristics that allow their structure to be modified and new analogs with different therapeutic properties to be generated. The objective of this research is to identify and select the C-7 heterocycle fluoroquinolone analog (**FQH 1-5**) with similar antibacterial activity in comparison with the reference fluoroquinolone through *in vitro*, *in silico* and *in vivo* evaluations. First, SAR analysis was done of the **FQH 1-5**, using an *in vitro* antimicrobial sensibility model, in order to select the best compound. Then, an *in silico* mechanism of action analysis was carried out by molecular docking. The cytotoxicity effect was evaluated in PBMCs cells. Finally, the antimicrobial potential was determined by an *in vivo* model of topical infection in mice. The results showed antimicrobial differences between the **FQH 1-5** and Gram-positive and Gram-negative bacteria, identifying the 7-benzimidazol-1-yl-fluoroquinolone (**FQH-2**) as the most active against *S. aureus*. Suggesting the same mechanism of action as the other fluoroquinolones; no cytotoxic effects on non-bacterial cells were found. **FQH-2** was demonstrated to decrease the amount of bacteria in infected wound tissue.

Keywords: Structure-Activity Relationship, Fluoroquinolone analogue, antimicrobial, *S. aureus*

Contenido

Análisis de estructura actividad de análogos de fluoroquinolonas y la evaluación antimicrobiana del 7-benzimidazol-1-il-fluoroquinolona en modelos <i>in vitro</i> , <i>in silico</i> e <i>in vivo</i>	v
1. Introducción.....	1
2. Objetivo.....	2
3. Materiales y Métodos.....	2
3.1 Síntesis química.....	2
3.2 Evaluación antimicrobiana.....	2
3.3 Acoplamiento molecular.....	2
3.4 Evaluación citotóxica del compuesto FQH-2.....	3
3.5 Evaluación del efecto antimicrobiano del FQH-2 en un modelo <i>in vivo</i> de infección tópica.....	3
3.6 Análisis estadístico.....	4
4. Resultados y Discusión.....	4
4.1 Síntesis química.....	4
4.2 Relación Estructura Actividad (REA) de los análogos de fluoroquinolonas FQH 1-5 frente bacterias Gram positivas y Gram negativas.....	4
4.3 Modelo <i>in silico</i> para confirmar la actividad antimicrobiana de los FQH 1-5 y el mecanismo de acción del FQH-2	5
4.4 Efecto no citotóxico del FQH-2 sobre células no bacterianas por el ensayo de citometría de flujo.....	5
4.5 Evaluación del efecto antimicrobiano del FQH-2 en un modelo <i>in vivo</i> de infección tópica con <i>S. aureus</i>	6
5. Conclusión.....	6
6. Referencias.....	6
Artículo experimental.....	7
Fluoroquinolone analogues SAR Analysis and the antimicrobial evaluation of 7-benzimidazol-1-yl-fluoroquinolone in <i>in vitro</i> , <i>in silico</i> , and <i>in vivo</i> models.....	7
Abstract.....	8
1. Introduction.....	9
2. Results and Discussion.....	11
3. Conclusion.....	21
4. Materials and methods.....	21
Figure Legends.....	30
References.....	31
Anexos.....	34
Supplementary Information.....	34
Binding energy score for docking calculations.....	35
FTIR – ATR spectra.....	36

NMR spectra	38
Thin Layer Chromatography.....	39

1. Introducción

La emergencia en salud sobre la resistencia a los antimicrobianos es un problema que la Organización Mundial de la Salud (OMS) ha estado resolviendo a través de diferentes medidas, como la emitida en 2017 por medio de la lista de bacterias con urgente necesidad de nuevos antibióticos, en la cual, clasifica a los microorganismos de acuerdo a su riesgo en: crítico, alto y medio. En la producción de nuevas moléculas con potencial antimicrobiano se debe considerar el diseño, la síntesis, la caracterización química y su actividad biológica. Por lo tanto, los estudios de Relación Estructura-Actividad (REA) son importantes para mejorar las propiedades de estructuras químicas conocidas como las fluoroquinolonas [1].

A partir de los estudios REA de las fluoroquinolonas se establece la correlación entre las diferentes posiciones de la estructura y sus efectos biológicos, con el objetivo de generar moléculas mejoradas. A continuación, se presenta una breve descripción de algunas posiciones importantes de las fluoroquinolonas. Las posiciones C-3 y C-4 conforman el farmacóforo de la molécula, ya que el grupo del ácido carboxílico en C-3 y el ceto en C-4 se conjuntan para formar el complejo metal-agua-aminoácidos (Serina, Aspartato y Glutamato) formando el aducto irreversible. En la posición C-6 está el átomo de flúor, que mejora la penetrabilidad de las quinolonas a la pared y membrana de bacterias Gram positivas y Gram negativas. La posición C-7 es el sitio flexible para introducir moléculas voluminosas capaces de modificar la actividad antimicrobiana. Para mantener el efecto antimicrobiano de la fluoroquinolona se recomienda que los sustituyentes en esta región deben conformar un enlace carbono-nitrógeno (C7-N) entre los átomos. Dentro de los grupos que mejoran la interacción con la proteína, son los heterociclos de tipo aromático o alifático, de cinco o seis átomos, con o sin ciclos fusionados que permiten incrementar el volumen [2].

Las fluoroquinolonas inhiben de manera dependiente e independiente a las enzimas ADN Topoisomerasa IIA (Topo II). Las enzimas Topo II están presentes en bacterias Gram positivas y Gram negativas, no obstante, la afinidad de las fluoroquinolonas es distinta, es decir, en las bacterias Gram-negativas actúan sobre la ADN girasa, mientras que para las Gram positivas es sobre la Topo IV. El objetivo terapéutico para ambas proteínas es semejante debido a que poseen el dominio tirosina y el ion Magnesio (Mg^{2+}), también la codificación de la secuencia de aminoácidos de esta región debe contener los aminoácidos (Serina, Aspartato y Glutamato) [3].

2. Objetivo

El objetivo del presente trabajo es identificar y seleccionar el análogo de fluoroquinolona con heterociclo en posición C-7 (**FQH 1-5**) con actividad antibiótica similar a la fluoroquinolona de referencia en evaluaciones *in vitro*, *in silico* e *in vivo*.

3. Materiales y Métodos

3.1 Síntesis química

Los análogos de fluoroquinolona con grupos de heterociclos amino en C-7 **FQH 1-5** se sintetizaron a partir del hidrólisis subsecuente del complejo borado en los análogos de fluoroquinolona **FQB 1-5** en medio básico para obtener las moléculas 3-carboxílico de las fluoroquinolonas siguientes: **FQH-1** (7-carbazol-1-il), **FQH-2** (7-benzimidazol-1-il), **FQH-3** (7-uracil-1-il), **FQH-4** (7-[5,5-difenil-hidantoina-1-il]) y **FQH-5** (Ácido 7-[2,6-dimetil-1,4-dihidropiridine-3,5-dicarboxílico]).

3.2 Evaluación antimicrobiana

Para el análisis de estructura actividad se evaluó por un modelo *in vitro*, mediante el ensayo de susceptibilidad antimicrobiana por microdilución en caldo en placa de 96 pozos de acuerdo al método reportado por el Clinical and Laboratory Institutes (CLSI) M07 11th edición M100 30th. En donde se determinó la Concentración Mínima Inhibitoria (CMI) y la Concentración Mínima Bactericida (CMB) del compuesto de referencia (ciprofloxacino: **CPX**), control de vehículo (solución acuosa) y los compuestos **FQH 1-5**. Para esta evaluación se utilizaron dos bacterias Gram-positivas *S. aureus* (ATCC 23235TM) y *E. faecalis* (ATCC 29212TM), y dos Gram-negativas: *E. coli* (ATCC 25922TM) y una cepa de *K. pneumoniae* de aislamiento clínico sensible a CPX, obtenida del separio del Laboratorio de Inmunotoxicología y terapéutica experimental.

3.3 Acoplamiento molecular

El modelo *in silico* se realizó para poder predecir su mecanismo de acción a partir de la semejanza de unión en el acoplamiento molecular de las moléculas **FQH 1-5** con ADN Topoisomerasa con el de referencia. Se descargaron las proteínas de las siguientes bacterias: *S. aureus*: 5cdq (ADN girasa), *K. pneumoniae*: 5eix (DNA Topo IV) y *E. coli*: 6rkv (ADN girasa) del Protein Data Bank (PDB). Se utilizó la estrategia de acoplamiento molecular basado en el ligando en el programa Autodock Vina. Excepto en la proteína de *E. coli* (6rkv) este tuvo una estrategia diferente, debido a sus características, se realizó un acoplamiento ciego (blind docking), y se confirmaron los sitios de interacción por medio del servidor Protein Plus. Por último, se realizaron todos los modelos de acoplamiento en el programa Pymol para

conocer las características de pose y orientación del ligando y los **FQH 1-5**. Para una mejor comprensión de los puntajes de la energía de unión se analizaron a través de un heat map usando el servidor Heatmapper.

3.4 Evaluación citotóxica del compuesto FQH-2

De acuerdo a la selección del compuesto con mejor efecto antimicrobiano, se probó el efecto citotóxico de dicho compuesto en células mononucleares de sangre periférica (PBMC's). Se obtuvieron las células por el método de separación de gradiente con Lymphoprep, y se determinó el número de células y viabilidad (<95%). Después se sembraron y expusieron las células a las condiciones de estudio: Sin estímulo (control de viabilidad), a una concentración de 4.39 μm de DMSO (control positivo), concentraciones tóxicas de ciprofloxacino 500 $\mu\text{g/ml}$ (control de referencia), solución acuosa de $\text{H}_2\text{O}/\text{NaOH}$ (control de vehículo) y concentraciones crecientes del **FQH** seleccionado; se incubaron por 24 h a 36 °C con 5% de CO_2 . Después se tiñeron las células de acuerdo a las instrucciones del fabricante del kit LIVE/DED™ Fixable Dead Cell Stain (Invitrogen, EUA). Por último, se midieron todas las muestras en un citómetro de flujo FACS CANTO II (BectonDickson, USA), y se analizaron con el programa FlowJo v 10.0 (BD, Bioscience, EUA).

3.5 Evaluación del efecto antimicrobiano del FQH-2 en un modelo in vivo de infección tópica

La evaluación del modelo *in vivo* de infección tópica tuvo la aprobación del Comité de Ética del Área de Ciencias de la Salud de la Universidad Autónoma de Zacatecas, con número de registro: ACS/UAZ182/2022 y se utilizó la NOM-062-Z00-199 para el manejo y cuidado de los animales de experimentación. Se utilizaron ratones Balb/c libres de patógenos con un rango de peso de 25 a 30g, Se separaron en cinco grupos (n=5): un grupo sin infección (non-infected). Los grupos de ratones con herida infectada fueron tratados de la siguiente manera: grupo sin tratamiento (NT), el grupo Ciprofloxacino (**CPX**) al 3% (Sophixin™ ungüento), el grupo vehículo (ungüento de solución acuosa) y el grupo con administración del ungüento de **FQH-2** al 3%. El ungüento de FQH-2 se preparó de manera aséptica con una base hidrofílica w/w, con carbapol, trietanolamina y una solución acuosa de FQH-2 al 3%, se integró en agitación constante y se almacenó a una temperatura ambiente

Las heridas quirúrgicas se infectaron de acuerdo al protocolo modificado de Mc Ripley y Within. Previo a la cirugía, se contaminaron las suturas con un inóculo de 2×10^9 UFC/mL de *S. aureus* (sensible a **CPX**) preparado en una solución estéril de 0.85% y ajustada por absorbancia. Al mismo tiempo se anestesiaron los animales, para posterior al afeitado y limpieza de la zona, se realizó la incisión longitudinal en el dorso del ratón. A las 5 h post-quirúrgicas en los grupos: **CPX**, Vehículo y

FQH-2 3% se administró la primera dosis de los ungüentos, las siguientes se dispensaron cada 12 h. Se siguieron a los animales por 5 días, en el último día fueron sacrificados con cámara de CO₂ en un ambiente libre de patógenos, recolectándose el tejido de herida. Posteriormente, se procesaron los tejidos para determinar la cantidad de bacterias. Se realizó una dilución seriada a partir del peso de la muestra para ajustar los volúmenes de solución salina estéril en la maceración de la herida, después, se tomó una muestra y se sembraron en placas Petri con agar sal y manitol, se incubaron por 24 h a 37 °C. Transcurrido el tiempo, se determinaron las UFC, se registraron los resultados para su posterior análisis.

3.6 Análisis estadístico

Todos los resultados experimentales se analizaron en programa Graph Pad Prism versión 8.0, en donde se realizaron pruebas de normalidad para después aplicar las pruebas de múltiples comparaciones entre los grupos por la prueba de ANOVA de una vía con post-test de Tukey. Los valores de diferencia significativa se consideraron desde * $p < 0.05$ hasta **** $p < 0.0001$ en todos los análisis.

4. Resultados y Discusión

4.1 Síntesis química

La síntesis de la forma activa de la fluoroquinolona es el ácido carboxílico en C-3, por la eliminación de difluoroboril mostró medianos a buenos rendimientos de reacción. Sólo la molécula **FQH-5** sufrió algunas modificaciones en la parte del heterociclo amínico unido en C-7 de la quinolona debido a la presencia de los grupos ésteres, los cuales en medio básico como con NaOH, las transformaciones de ácido carboxílico fueron observadas y confirmadas por ¹H NMR [4].

4.2 Relación Estructura Actividad (REA) de los análogos de fluoroquinolonas **FQH 1-5** frente bacterias Gram positivas y Gram negativas

El resultado de la prueba de susceptibilidad antimicrobiana demuestra que la bacteria de *E. coli* es la que presenta susceptibilidad frente a todos los compuestos debido a que tiene menores CMI de la serie de bacterias (ver Tabla 1), sin embargo, ninguna de ellas es cercana al de referencia (**CPX**).

El análisis de la REA muestra la variabilidad de la estructura química en cada una de los heterociclos amínicos unidos a C-7 **FQH 1-5**. Se distinguen dos grupos principales: 1) Aquellos que presentan carbonilos en el heterociclo, tales como **FQH-3, 4 y 5**, los cuales mostraron valores de CMI mayores a las de referencia (**CPX**) (>128 µg/mL), principalmente en bacterias Gram-positivas. 2) Los que tienen

anillos fusionados, como **FQH-1** y **2**, en donde se observó que los valores de CMI fueron menores que los anteriores para las bacterias Gram negativas, mientras que para las Gram positivas tuvieron valores cercanos al estándar (**CPX**: 0.250 µg/mL), especialmente el **FQH-2** y específicamente sobre el *S. aureus* (0.5 µg/mL). Por lo tanto, proponemos que los cambios estructurales influyen en la actividad antimicrobiana, posiblemente por su carácter aromático, donde se pueden organizar de menor a mayor efecto antibiótico, respecto a su cercanía con el **CPX**, de la siguiente manera **FQH-5<FQH-3<FQH-4<FQH-1<FQH-2**. Además, la afinidad por los tipos bacterianos, donde los más aromáticos (**FQH-1** y **2**) tuvieron mayor sensibilidad antimicrobiana por las bacterias Gram-positivas, identificando al **FQH-2** como el compuesto líder por tener efectos inhibitorios semejantes al **CPX** en la bacteria *S. aureus* [2].

4.3 Modelo *in silico* para confirmar la actividad antimicrobiana de los **FQH 1-5** y el mecanismo de acción del **FQH-2**

En las predicciones del modelo *in silico*, se observan similitudes con los resultados experimentales, por lo que permite confirmar al **FQH-2** como el compuesto líder, debido a que presenta valores muy cercanos al de referencia (Moxifloxacino -11.3 kcal/mol Vs **FQH-2** -10.6 kcal/mol) en la proteína de *S. aureus* (5cdq). Por lo tanto, cuando se analiza la orientación del acoplamiento entre el **FQH-2** y la proteína, se muestra que existe una amplia área de contacto con varios aminoácidos como ARG 122, GLY 459, GLU 585 y ASP 437, en donde algunos coinciden con el de referencia. Por lo que se podría decir que el **FQH-2** probablemente actúa en el mismo sitio que las fluoroquinolonas de referencia. Además, al superponer las dos estructuras químicas de **FQH-2** y Moxifloxacino, se observa una superposición muy semejante, sin embargo, en la región C-7 se muestra un ligero desplazamiento, que se atribuye a las características del heterociclo sustituyente. Esta diferencia puede deberse a la planaridad de estos grupos sustituyentes [2]. En el Moxifloxacino presenta un heterociclo de tipo aza-biciclo que tiene una rotación limitada en el enlace sigma entre el átomo de nitrógeno del aza-biciclo y el carbono del C-7 en la fluoroquinolona, debido al impedimento estérico que proporciona el metoxi en C-8. Mientras que el **FQH-2** no posee sustituyentes en C-8, permitiendo la torsión de rotación con más grados de libertad, donde la orientación preferente del grupo benzimidazol-1-il es perpendicular al plano de la quinolona, esto podría ser la causa de las diferencias en el efecto antimicrobiana, aunque, se requieren estudios más detallados para confirmarlo [2, 3].

4.4 Efecto no citotóxico del **FQH-2** sobre células no bacterianas por el ensayo de citometría de flujo

Ya que se ha seleccionado el **FQH-2**, se continúa con la evaluación citotóxica en células PBMC's, donde se demostró que este compuesto no aumenta el porcentaje de células muertas de cultivos

expuestos a concentraciones crecientes (4µg/mL-128µg/mL) del **FQH-2**. A diferencia del **CPX** (no de manera estadísticamente significativa) si causó mortalidad de las células, lo cual ya se había reportado en otros trabajos la inhibición del ADN Topoisomerasa II [5]. Al no mostrar efectos nocivos sobre estas células, es posible su actividad selectiva únicamente por las ADN Topo II de las bacterias, por lo que se sugiere que no tienen riesgo su uso en modelo *in vivo*.

4.5 Evaluación del efecto antimicrobiano del **FQH-2** en un modelo *in vivo* de infección tópica con *S. aureus*

En la evaluación del modelo de infección *in vivo* se demuestra la capacidad de la bacteria *S. aureus* de causar patrones morfológicos de la infección en las heridas quirúrgicas de los grupos infectados frente al no infectado. Posteriormente cuando se analiza la variación de la cantidad de bacteria en los tejidos de los grupos experimentales infectado sin tratamiento con los que tuvieron administración del ungüento, se observa la disminución estadísticamente significativa en el porcentaje de UFC/mL en el grupo de **CPX** al 3% (13.08% ±19.52) y el **FQH-2** al 3% (21.08% ± 27.38). Esta actividad, revela el potencial del compuesto **FQH-2** como agente antimicrobiano para las infecciones de *S. aureus*.

5. Conclusión

Por medio de la evaluación REA de los análogos de fluoroquinolona **FQH 1-5** se demostró que los heterociclos aromáticos fusionados en posición C-7 mejoran la susceptibilidad antimicrobiana en bacterias Gram-negativas y principalmente en las Gram positivas. El compuesto **FQH-2** fue el mejor compuesto contra *S. aureus*. Demostrando no tener actividad citotóxica en células no bacterianas. Y se comprobó su efecto antimicrobiano con la disminución de las UFC en el modelo *in vivo* de infección tópica con *S. aureus*. Además, durante la evaluación antimicrobiana mediante los diferentes modelos experimentales, se encontró reproducibilidad en la cercanía de la actividad inhibitoria entre el **FQH-2** y el ciprofloxacino. Se recomienda que futuras investigaciones se dirijan en la evaluación sobre cepas resistentes.

6. Referencias

1. Organization World Health. *WHO publishes list of bacteria for which new antibiotics are urgently needed, 2017*. Geneva: Switzerland. Communications Office. Recuperado de: <https://www.who.int/news/item/27-02-2017-who-publishes-list-of-bacteria-for-which-new-antibiotics-are-urgently-needed>
2. Peterson, L.R. (2001). Quinolone Molecular Structure-Activity Relationships: What We Have Learned about Improving Antimicrobial Activity. *Clin Infect Dis*. 2001. **33**(3), S180-S186.
3. Pham, T. D. M., et al. (2019). Quinolone antibiotics. *Med Chem Comm* 10(10), 1719-1739.
4. Hernández-López, H., et al. (2019) Synthesis of Hybrid Fluoroquinolone-Boron Complexes and Their Evaluation in Cervical Cancer Cell Lines. *Journal of Chemistry*, 1-6.
5. Azéma, J., et al. (2009) 7-((4-Substituted)piperazin-1-yl) derivatives of ciprofloxacin: synthesis and in vitro biological evaluation as potential antitumor agents. *Bioorg Med Chem*, 17(15), 396-407.

Artículo experimental

Fluoroquinolone analogues SAR Analysis and the antimicrobial evaluation of 7-benzimidazol-1-yl-fluoroquinolone in *in vitro*, *in silico*, and *in vivo* models

Medellín-Luna Mitzzy Fátima,^{1,2,3} Hernández-López Hiram,² Castañeda-Delgado Julio Enrique,^{3,4} Martínez-Gutierrez Fidel,¹ Lara-Ramírez Edgar,³ Espinoza Rodríguez Joan Jair,² García- Cruz Salvador,⁴ Portales-Pérez Diana Patricia,¹ Cervantes-Villagrana Alberto Rafael.²

- 1 Doctorado en Ciencias Farmacobiológicas, Facultad de Ciencias Químicas, Universidad Autónoma de San Luis Potosí, 78210 San Luis Potosí, México.
- 2 Unidad Académica de Ciencias Químicas, Universidad Autónoma de Zacatecas, 98160, Zacatecas, México.
- 3 Unidad de Investigación Biomédica de Zacatecas, Instituto Mexicano del Seguro Social, 98000, Zacatecas, México.
- 4 Investigadores por México, CONAHCYT, Consejo Nacional de Humanidades, ciencias y tecnologías, 03940 Ciudad de México. México
- 5 Departamento de Cirugía experimental e Investigación Quirúrgica y Bioterio. “Claude Bernard”. Área de Ciencias de la Salud. Universidad Autónoma de Zacatecas, 98160, Zacatecas, México.

Corresponding author: Cervantes-Villagrana Alberto Rafael PhD

e-mail: dr.albertocervantes@uaz.edu.mx

[Address: Campus universitario siglo XXI, edificio S cubículo 14. Carretera Zacatecas-Guadalajara km 6. Colonia ejido “La escondida”. Zacatecas, Zac. México. CP 98160](#)

Abstract

Structure Activity Relationship (SAR) studies allow the evaluation of the relationship between structural chemical changes and biological activity. Fluoroquinolones have chemical characteristics that allow their structure to be modified and new analogs with different therapeutic properties to be generated. The objective of this research is to identify and select the C-7 heterocycle fluoroquinolone analog (**FQH 1-5**) with antibacterial activity similar to the reference fluoroquinolone through *in vitro*, *in silico* and *in vivo* evaluations. First, SAR analysis was done of the **FQH 1-5**, using an *in vitro* antimicrobial sensibility model, in order to select the best compound. Then, an *in silico* model mechanism of action analysis was carried out by molecular docking. The non-bacterial cell cytotoxicity was evaluated and finally, the antimicrobial potential was determined by an *in vivo* model of topical infection in mice. The results showed antimicrobial differences between the **FQH 1-5** and Gram-positive and Gram-negative bacteria, identifying the 7-benzimidazol-1-yl-fluoroquinolone (**FQH-2**) as the most active against *S. aureus*. Suggesting the same mechanism of action as the other fluoroquinolones; no cytotoxic effects on non-bacterial cells were found. **FQH-2** was demonstrated to decrease the amount of bacteria in infected wound tissue.

Keywords: Structure-Activity Relationship, Fluoroquinolone analogue, antimicrobial, *S. aureus*.

1. Introduction

Over the last few decades, the World Health Organization (WHO) has considered antimicrobial resistance (AMR) as an urgent public health problem [1], establishing strategies for its remediation [2, 3]. One of these strategies is the development of new antibiotics focused on microorganisms classified as critical, high, and medium risk [4]. An estimated 13.7 million deaths worldwide are related to infections with AMR strains, where *S. aureus* is the microorganism responsible for more than 1 million deaths, followed by *E. coli*, *S. pneumoniae*, *K. pneumoniae* and *P. aureginosa* with 500,000 deaths [5].

The structural design of new chemical molecules with possible antimicrobial effect is guided by the structure of existing antibiotics with the purpose of improving their pharmacodynamic and pharmacokinetic properties [6, 7]. However, these molecules must be studied during the different experimental phases including synthesis, chemical characterization and biological activity [8]. To do this, Structure-Activity Relationship (SAR) evaluations [9] are carried out, such as Computer Aided Drug Design (CADD) through molecular docking [10]. The advantage of these CAAD techniques is the time and cost reduction for the synthesis processes, biological evaluations, and research [11].

In different SAR studies, fluoroquinolones have described the correlation between the different positions within the quinolone ring and their biological effects [12], facilitating the design of new molecules, thus producing hybrids, derivatives or analogues [13, 14]. The following is a brief description of the SAR of the structure of fluoroquinolones. In the C-1 position there is a nitrogen atom (N1), so the insertion of cyclic groups generally favors antimicrobial potency. The C-3 and C-4 positions make up the pharmacophore of the molecule, since the carboxylic acid group at C-3 and the keto group at C-4 come together to form the metal-water-amino acid complex, through hydrogen and salt bridges between the oxo groups of these positions and the amino acids: Serine, Aspartate and Glutamate form the irreversible adduct, known as the Quinolone Resistance Determining Region (QRDR). The fluorine atom is in position C-6 which improves the penetrability of quinolones through the wall and membrane of Gram-positive and Gram-negative bacteria [15, 16].

The C-7 position is the flexible site to introduce bulky molecules capable of modifying antimicrobial activity [15, 17]. To maintain the antibiotic effect of fluoroquinolone, it is recommended that the substituents in this region should form a carbon-nitrogen bond (C7-N) between the atoms. Within the groups that improve the interaction with the protein, are the heterocycles of the aromatic or aliphatic type, of five or six atoms, with or without fused cycles that allow volume increase [18]. At present, the increased microbial susceptibility to both types of bacteria of fluoroquinolones with heterocycles such as pyrimidine, indole or imidazole has been demonstrated [15, 18, 19].

Fluoroquinolones dependently and independently inhibit DNA Topoisomerase IIA (Topo II) enzymes [20]. The dependent pathway is through the formation of the metal-water-amino acid complex previously mentioned; the independent pathway is through the formation of stacking bonds with DNA structures, although this is a hypothesis [21-23]. By forming the aforementioned interactions, the tension of the supercoiled DNA strands originated by helicase activity during replication is increased, generating SOS signals of bacterial death [20-23]. Topo II enzymes are present in Gram-positive and Gram-negative bacteria, however, the affinity of fluoroquinolones is different for each type of bacteria, that is, in Gram-negative bacteria, fluoroquinolones act on DNA gyrase, while for Gram-positive, on Topo IV [24]. The therapeutic target for both proteins is similar because they have the tyrosine domain and the Magnesium ion (Mg^{2+}). In addition, the amino acid sequence encoding this region must contain the amino acids QRDR (Serine, Aspartate and Glutamate) [23, 24].

The aim of this study was to identify and select the fluoroquinolone analog with heterocycle in position C-7 (**FQH 1-5**) with antibiotic activity similar to the reference fluoroquinolone in evaluations *in vitro*, *in silico* and *in vivo*. From a SAR analysis of the five **FQH 1-5** fluoroquinolone analogues obtained by chemical synthesis, an evaluation was carried out *in vitro* of antimicrobial sensitivity, through which the compound with antibiotic activity similar to that of the reference compound in Gram-positive and Gram-negative bacteria is identified; subsequently, its mechanism of action is predicted in a model *in silico* by molecular docking. Its cytotoxic effect on non-bacterial cells is then determined and finally, its antimicrobial effect is evaluated in a *in vivo* model of topical infection in mice.

2. Results and Discussion

2.1 Synthesis and chemical evaluation

Fluoroquinolone analogs with heterocycles at C-7 position **FQH 1-5** were synthesized from the hydrolysis of compounds **FQB 1-5**. The introduction of a weak nucleophilic agent such as amino heterocycles: uracil, benzimidazole, tetrahydro-carbazole, 1,4-dihydropyridine and 5,5-diphenyl-hydantoin, was only possible with the formation of the boron complex with fluoroquinolone, as described by *Miranda-Sánchez, et al.* [25] (see **Figure 4**). However, as the active form of the fluoroquinolone is the carboxylic acid at the C-3 position, the removal of the difluoroboryl part was carried out through basic hydrolysis with the use of NaOH (2N), showing medium to good reaction yields. Only the **FQH-5** molecule underwent some modifications in the part of the amino heterocycle linked at C-7 of the quinolone due to the presence of ester groups. The carboxylic acid transformations were observed and confirmed by ¹H NMR in a basic medium such as NaOH.

In the present investigation, only the antimicrobial activity of the **FQH 1-5** hydrolyzed compounds was evaluated, because previous trials predicted a better outlook than **FQB 1-5**. In addition, there is little evidence regarding boronated fluoroquinolone complexes as antimicrobials; therefore, their evaluation in the different experimental models of the work was ruled out.

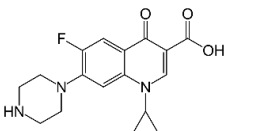
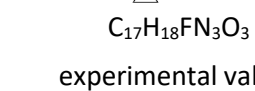
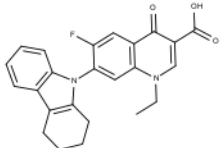
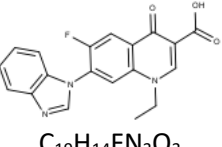
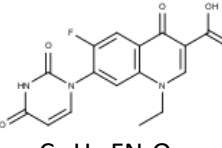
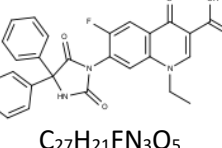
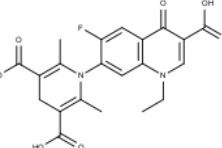
2.2 Structure activity relationship (SAR) of the fluoroquinolone analogs FQH 1-5 against Gram-positive and Gram-negative reference bacteria

The SAR of fluoroquinolone analogues **FQH 1-5** was determined based on the antimicrobial effect obtained from the MIC and the MBC evaluated against the reference Gram-positive strains *S. aureus* and *E. faecalis*, as well as the Gram-negative strain *E. coli* and the strain of the clinical isolate *K. pneumoniae*. Additionally, the Ciprofloxacin (**CPX**) patent formulation was used as a reference control and for the standardization of the method used in this work by which the standard values of the concentrations of MIC and MBC on each of the bacterial strains were defined. The MIC data obtained is close to the reference values reported by the CLSI for each bacterial strain: *S. aureus* (0.250 mg/mL Vs 0.125-0.5 mg/mL), *E. faecalis* (0.250 mg/mL Vs 2-0.250 mg/mL), *E. coli* (0.013 mg/mL Vs 0.016-0.004 mg/mL) y *K. pneumoniae* (0.5 mg/mL Vs <1 mg/mL), as shown in **table 1**. Therefore, the method used to demonstrate antibacterial susceptibility to **FQH 1-5** is suitable for standard bacterial strains.

In **table 1**, the MIC and MBC values of the reference compound are shown: ciprofloxacin (**CPX**) and the **FQH 1-5** for the description of the SAR between the heterocycle changes in each structure and the microbial susceptibility in each reference strain. The results demonstrated differences in the antimicrobial sensitivity of the **FQH 1-5** analogues, where the bacterium *E. coli* maintains a marked

susceptibility to each of the molecules, though concentrations close to those of **CPX** were not reached in any compound.

Table 2. MIC and MBC values of reference fluoroquinolone (**CPX**) and fluoroquinolone analogs **FQH 1-5**

Label	Structure	<i>S. aureus</i> (ATCC 25923)		<i>E. feacalis</i> (ATCC 29212)		<i>E. coli</i> (ATCC 25922)		<i>K. pneumoniae</i> *	
		MIC (mg/mL)	MBC (µg/mL)	MIC (µg/mL)	MBC (µg/mL)	MIC (µg/mL)	MBC (µg/mL)	MIC (µg/mL)	MBC (µg/mL)
CPX	CLSI Values  <chem>C17H18FN3O3</chem> experimental values	0.125-0.5	0.250	0.250-2	0.250	0.016-0.004	0.008	<1	1
	 <chem>C17H18FN3O3</chem> experimental values	0.250	0.250	0.250	0.250	0.013 ± 0.005 ^a	0.033 ± 0.002 ^a	0.5	0.5
FQH-1	 <chem>C24H21FN2O3</chem>	32	>128 ^b	128 ^b	>128 ^b	1.667 ± 0.577 ^a	4	64	64
FQH-2	 <chem>C19H14FN3O3</chem>	0.5	0.5	4	4	1.333 ± 0.577 ^a	2	16	32
FQH-3	 <chem>C16H12FN3O5</chem>	128	128	128	>128 ^b	1.667 ± 0.577 ^a	4	128	128
FQH-4	 <chem>C27H21FN3O5</chem>	128	>128	128	>128 ^b	2	4	32	32
FQH-5	 <chem>C21H22FN2O7</chem>	128	>128 ^b	128	>128 ^b	4	4	64	64

^aVariance caused by the scope of the technique with no statistically significant differences.

^bValues greater than the concentrations reached by the solubility in the aqueous medium NaOH/H₂O

In the analysis of the SAR, the chemical structural variability of each amino heterocycle attached to C-7 of the fluoroquinolone was reviewed and two groups were detected: 1) those that present carbonyls in the heterocycle, such as **FQH-3, 4** and **5**, which showed MIC values higher than the reference (**CPX**) (>128µg/mL), mainly in Gram-positive bacteria. And 2) those with fused rings, like **FQH-1** and **2**, where it was observed that the MIC values were very close to the standard used on Gram-negative bacteria, as well as on Gram-positive strains, obtaining concentrations of 32 µg/mL and 0.5 µg/mL for **FQH-1** and **FQH-2**, respectively. It is possible that the differences in the resulting MIC values have a close relationship with the binding of the aromatic heterocycle at C-7 of the fluoroquinolone, providing greater stability in the molecule due to electron conjugation and inducing a shift in electron density towards the carboxylic acid and keto group at C-3 and C-4, respectively. As compared to the tetrahydro-carbazole heterocycles in **FQH-1** and benzimidazole in **FQH-2**, both presented a dominant susceptibility to inhibit Gram-negative strains, having MIC and MBC values lower than those of the compounds **FQH 3-5**. Also, the **FQH-2** showed MIC values similar to those of CPX against *S. aureus* (0.250 µg/ml vs. 0.500 µg/ml). For this reason, a possible relationship is assumed between the aromatic heterocycles and how “bulky” the substitution attached to C-7 of fluoroquinolone trough to improve interaction with the enzyme for bacterial inhibition. It is proposed that the decrease in aromatic character could be directly proportional to the antimicrobial effect presented in fluoroquinolones, such as in the case of **FQH-1**, in which the antimicrobial susceptibility decreases, compared to the **FQH-2** which is very similar to the standard; however, it is necessary to carry out a detailed mechanistic evaluation to confirm this hypothesis, which is not the object of study for the present work.

SAR evaluations previously reported in the literature for fluoroquinolones describe the influence of amino heterocycles made up of five or more carbon atoms joined at C-7 of the quinolone and the importance of improving and expanding the antimicrobial effect of quinoline derivatives [12, 19, 26]. Based on the above and according to their bacterial inhibition effect observed in the present work, some insights could be inferred: the fused heterocycle presented a broad spectrum of bacterial inhibition, acting mainly on *S. aureus*; likewise, a correlation was observed between the increase in aromatic character and bacterial inhibition, as in the case of **FQH-2**. This description is a suggested proposal in accordance with the results of this work, since at present this type of structure has not been described. On the other hand, benzimidazole linked to fluoroquinolones has been studied through quinolone hybrids in N-1 [27] and its antimicrobial activity in reference strains (similar to those evaluated here) and in wild strains. However, comparing the results of these hybrids and the analogues of this work, it is found that the binding of benzimidazole is favored in C-7 of the fluoroquinolone more than in N-1, due to the fact that the antimicrobial action is improved against *S. aureus*. In summary, the structural changes that influence the antimicrobial activity in heterocycles are defined according to aromaticity,

where they can be organized from lowest to highest antibiotic effect, according to the proximity to the reference values (**CPX**) of the following manner: **FQH-5**<**FQH-3**<**FQH-4**<**FQH-1**<**FQH-2**. In addition, the affinity for bacterial types, where the aromatics (**FQH-1** and **2**) had greater antimicrobial sensitivity by Gram-positive bacteria, identified the **FQH-2** as the leading compound for having inhibitory effects similar to **CPX** in the bacterium *S. aureus*. Therefore, evaluating the molecular patterns of binding with the Topo II protein provides evidence regarding the possible mechanism of action.

2.3 *In silico* model by molecular docking to confirm the antimicrobial activity of FQH 1-5 and the mechanism of action of FQH-2

As mentioned, CADD tools such as molecular docking [11] provide the opportunity to expand SAR studies of the contacts between the chemical structure under study with the different protein components, such as amino acids or catalytic ions present in the active site or "pocket" [10, 26]. Therefore, it is possible through molecular docking to interpret and predict whether ligand-receptor binding is feasible by means of stability calculations (scores) in terms of binding energies (expressed in terms of Gibbs free energy, ΔG) [28]. In SAR studies in which molecular docking is used to screen molecules as derivatives of fluoroquinolones, by selecting the chemical structures that present the best ΔG values, the MICs for each derivative were subsequently verified. Our results demonstrated that heterocycles larger than six atoms enhance the inhibitory activity of both Gram-positive and Gram-negative bacteria [19, 26]. This is further supported by previous data from other groups where fluoroquinolone derivatives with heterocycle amine in C-7 and chlorine atom in C-8 (**FQP-30**), *in vitro* studies (MIC) showed enhanced antibiotic activity [29]. However, when bringing the results to the *in silico* plane by molecular docking, they were found to be discordant, because the orientation and pose were different from the reference [30]. The mechanistic details of such SAR analysis awaits for experimental evidence.

Among the applications of molecular docking is the prediction of antimicrobial activity which could support the mechanism of action of these molecules derived from fluoroquinolones [31]. Therefore, in the present investigation a screening model was proposed *in silico*, focused on discerning those quinoline derivatives that project the greatest antimicrobial activity of fluoroquinolone analogues **FQH 1-5**. First the pocket coordinates for each of the bacteria were corroborated, calculating the RMSD (data not shown) of the ligand-receptor model co-crystallized with Moxifloxacin (**MXF**) and the experimental molecular docking model. Our results show similar values between both models, being interpreted as precise coordinates for the location of the pocket. Furthermore, these binding energy score values are used as a reference in future comparisons with fluoroquinolone analogues **FQH 1-5**. In **Figure 1**, the results of the molecular docking of the **FQH 1-5** are shown with the different Topo II proteins from various bacterial strains showing the binding energy score through a heat map (**see Figure 1A**), where each

cell represents the binding energy score value expressed in kcal/mol for each **FQH 1-5** and its respective Topo II protein. A red cell represents more negative energy values (greater ligand-receptor binding stability), while blue cells show lower ligand-receptor binding stability. Therefore, the results obtained from the calculated interactions between **FQH-1** and **FQH-2** with the different target proteins, present uniformity of red cells, with scores close to those of the reference. These results agree with the antimicrobial activity evaluated in the *in vitro* model, where **FQH-1** and **FQH-2** were the ones with the highest antimicrobial activity against Gram-positive and Gram-negative bacteria as previously shown in table 1.

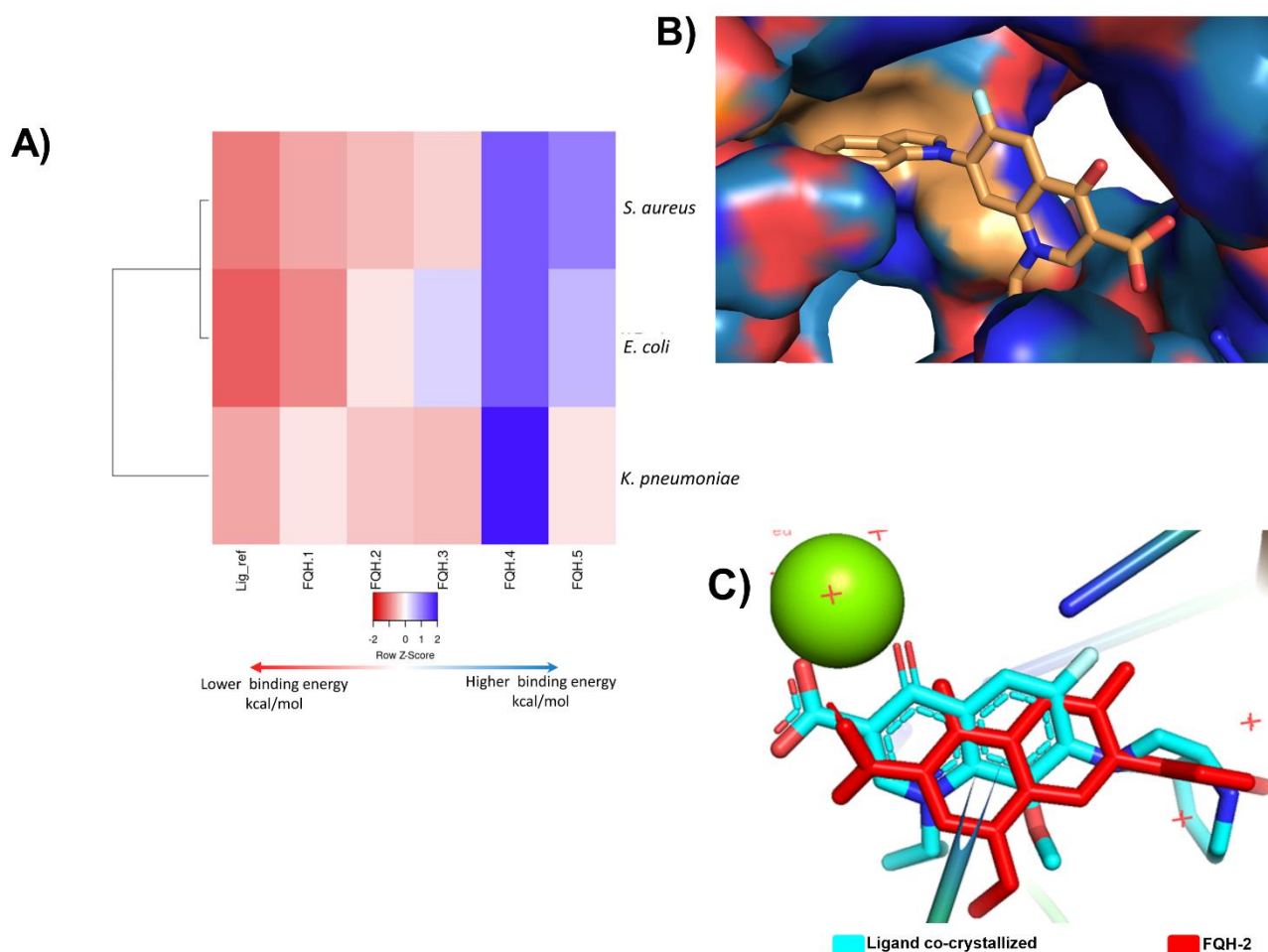


Figure 1. Molecular docking analysis of FQH-2 with Topoisomerase II from several bacterial strains

Next, we sought to model the orientation of the **FQH-2** inside the protein pocket of the *S. aureus* to propose a possible mechanism of action. The evaluation of the contact surface of the **FQH-2** in the DNA gyrase *S. aureus* (**Figure 1B**), shows a broad interaction with the cleavage site amino acids (orange color) such as ARG 122, GLY 459, GLU 585, and ASP 437, in addition to demonstrating that the ligand pose of the **FQH-2** and **MXF** (reference) are very similar (**see Figure 1C**). The slight differences found in the orientation between the **FHQ-2** and **MXF** are based on the heterocycle linked to C-7 of quinolone, and are attributed to the property of planarity provided by benzimidazole with respect to the **MXF** bicycle, to the influence on the final pose [19]. The heterocycle attached to the C-7 of Moxifloxacin is of the aza-bicycle type that has limited rotation at the sigma bond between the aza-bicycle nitrogen atom and the C-7 carbon in the fluoroquinolone, due to the steric hindrance provided by the methoxy at C-8 [32]. The **FQH-2** does not have substituents at C-8, allowing rotational torsion with more degrees of freedom, where the preferred orientation of the benzimidazol-1-yl group is perpendicular to the plane of the quinolone. To summarize, a structural property that affects the pose or orientation of the molecule in the biological target is planarity, where having substituent groups with double bonds near the groups at C-7 will limit the rotation of the latter and hence their stability of interaction at the site of action.

As mentioned, the C-7 position in the fluoroquinolone is key to modifying the structure and increasing the stability of the interaction with the protein. In the design of molecules **FQH 1-5**, changes in amino heterocycle in C-7 have shown differences in their biological activity. These are confirmed by the *in silico* model, where the results of the chosen compound **FQH-2** were very close to the reference (Moxifloxacin -11.3 kcal/mol Vs **FQH-2** -10.6 kcal/mol), a pattern resembling that of the *in vitro* results. This effect can be explained by the heterocycle (at C-7) characteristics which allow the displacement of the electronic density on the functional groups at C-3 and C-4, substantially modifying the interactions with the amino acids in the “pockets”. Therefore, these results strongly suggest that the compound 7-benzimidazol-1-yl-fluoroquinolone as the optimal compound, in addition to proposing that **FQH-2** may present the antimicrobial mechanism of action by inhibiting Topo II; however, verification through biological assays is suggested. In addition, the evaluation on non-bacterial cells is necessary to rule out effects on Topo II proteins in general and to recognize the bacterial selectivity of the **FQH-2**.

2.4 Non-cytotoxic effect of FQH-2 on non-bacterial cells by flow cytometry assay

One of the pharmacodynamic properties of fluoroquinolones is that they act selectively against bacteria and other microorganisms rather than against human cells, due to the fact that even though prokaryotic (bacterial) and eukaryotic (human) Topo II DNA proteins are similar, the amino acid sequence of the catalytic (or cleavage) site is different [15], which suggests that the affinity of the fluoroquinolones is different and that they act preferentially in prokaryotic cells.

Collectively, our results show that the molecule 7-benzimidazol-1-yl-fluoroquinolone (**FQH-2**) inhibits the Topo II bacterial enzyme; however, this enzyme is also present in non-bacterial cells. In addition, the benzimidazole molecule[33] has been shown to have antimicrobial activity [34], as well as antitumor[35], antiviral [36], and antifungal [37] activity. For this reason, the evaluation of cytotoxicity in non-bacterial cells is relevant. Consequently, it was necessary to determine if the **FQH-2** did not have toxic effects in eucariotic or mammalian cells. To evaluate the cytotoxic effects of drugs or xenobiotics, it is necessary to use complex cells that may have a greater or constant exposure to them [38]; in this sense, peripheral blood mononuclear cells (PBMCs) are very useful cells for evaluating cytotoxic responses. In this work, the cytotoxic response of the mononuclear cells to **FQH-2** was evaluated by flow cytometry in a Propidium Iodide based assay. We used a concentration range of 128 to 4 $\mu\text{g/ml}$ (8-fold higher than the MIC obtained for *S. aureus*). The result of the distribution of the cell populations according to their condition can be observed in the histogram of **Figure 2A**, where the highest number of dead cells obtained were those exposed to DMSO (positive control), resulting in the highest fluorescence damage to Propidium Iodide histogram, while for those exposed to **FQH-2**, the fluorescence amounts were lower, indicating low toxicity and the presence of viable cells. On the other hand, the mortality percentage data (**Figure 2B**) shows the non-cytotoxic effects of the different evaluated conditions, such as the one without stimulus (NS) that showed low levels of mortality (<5%). The cells exposed to CPX obtained a mortality <20% higher than that of the NS control, while for **FQH-2** exposure, the mortality rates were lower than DMSO and CPX exposure for all concentrations.

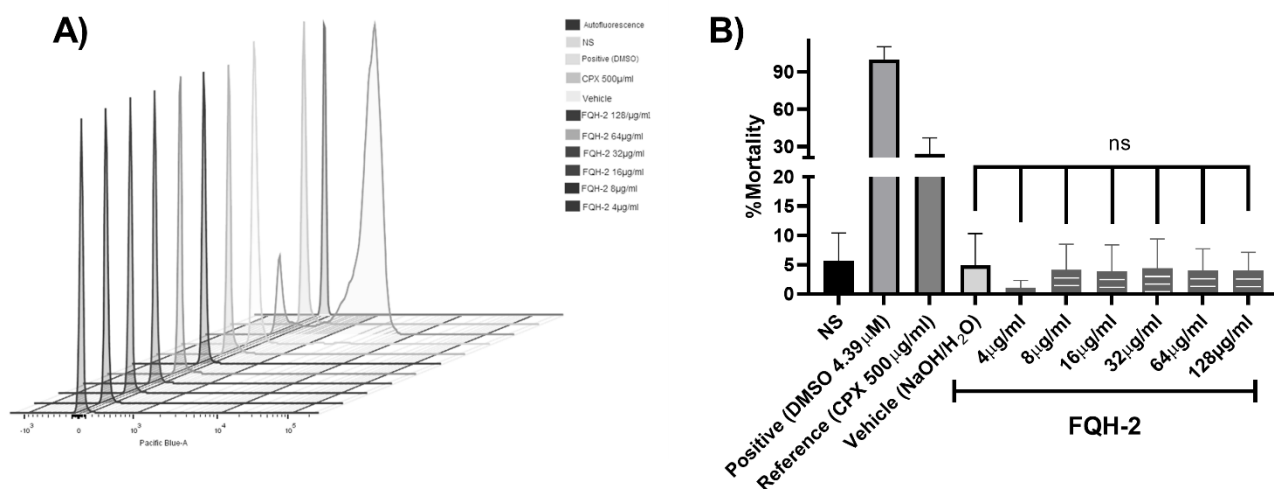


Figure 2. Non-cytotoxic effect of FQH-2 in peripheral blood mononuclear cells.

Based on these results, the **FQH-2** demonstrates low cell toxicity, we suggest that this may be due to low affinity for Topo II DNA from non-bacterial cells. Based on reports of cytotoxic studies of the CPX (IC₅₀) [39], where the decrease in HeLa cell viability is demonstrated by the Topo II DNA inhibition [40, 41]. We show that despite using higher concentrations of the **FQH-2**, effects similar to those of the NS control were obtained, which indicates that **FQH-2** has no cytotoxic effect on blood cells of PBMCs and suggests a minimum risk of use in animal models.

2.5 Evaluation of the antimicrobial effect of FQH-2 in a mouse model of topical infection with *S. aureus*

According to the previous results, the **FQH-2** is the leading compound with the best antimicrobial activity against *Staphylococcus aureus*, which is an etiological and pathogenic agent of skin infections that could lead to a lethal disease such as impetigo [42, 43]. Similarly, *S. aureus* is reported as the most common infectious agent in surgical site infections [44]. Therefore, we designed an *S. aureus* infection in surgical wounds to evaluate the antimicrobial effects of **FQH-2**. A hydrophilic base ointment containing **FQH-2** at 3% w/w was used. This had a homogeneous appearance of transparent color and colloidal consistency that favored easy application on contaminated surgical wounds. In addition, it was confirmed that this vehicle base did not influence bacterial inhibition or proliferation in comparison with others base of vehicles (data not show).

The *in vivo* model of skin infections of surgical wounds in mice was shown to have the morphopathological features of contamination by *S. aureus*, causing physiological changes in the area associated with the infection. The physiopathological alterations are closely related to the inflammatory process, such as the formation of edema, reddening of the skin and purulent discharge, as well as changes in the amount of bacteria present in the wound [45]. The experimental follow-up was five days later. In **Figure 3A**, representative images of the *in vivo* model are shown for topical infections of the experimental groups from day 1 (beginning) and day 5 (end). The first column contains the photos of the uninfected group, where a typical lesion pattern is observed on day 1; on day 5, the patterns of the lesion without bacterial contamination are observed, where no edema is seen throughout the tissue (identified with a continuous red arrow), just as the edges of the wound (discontinuous red arrow) are facing each other, which indicates that the correct healing process was taking place. Finally, no purulent secretions were observed, confirming that this group did not present infection.

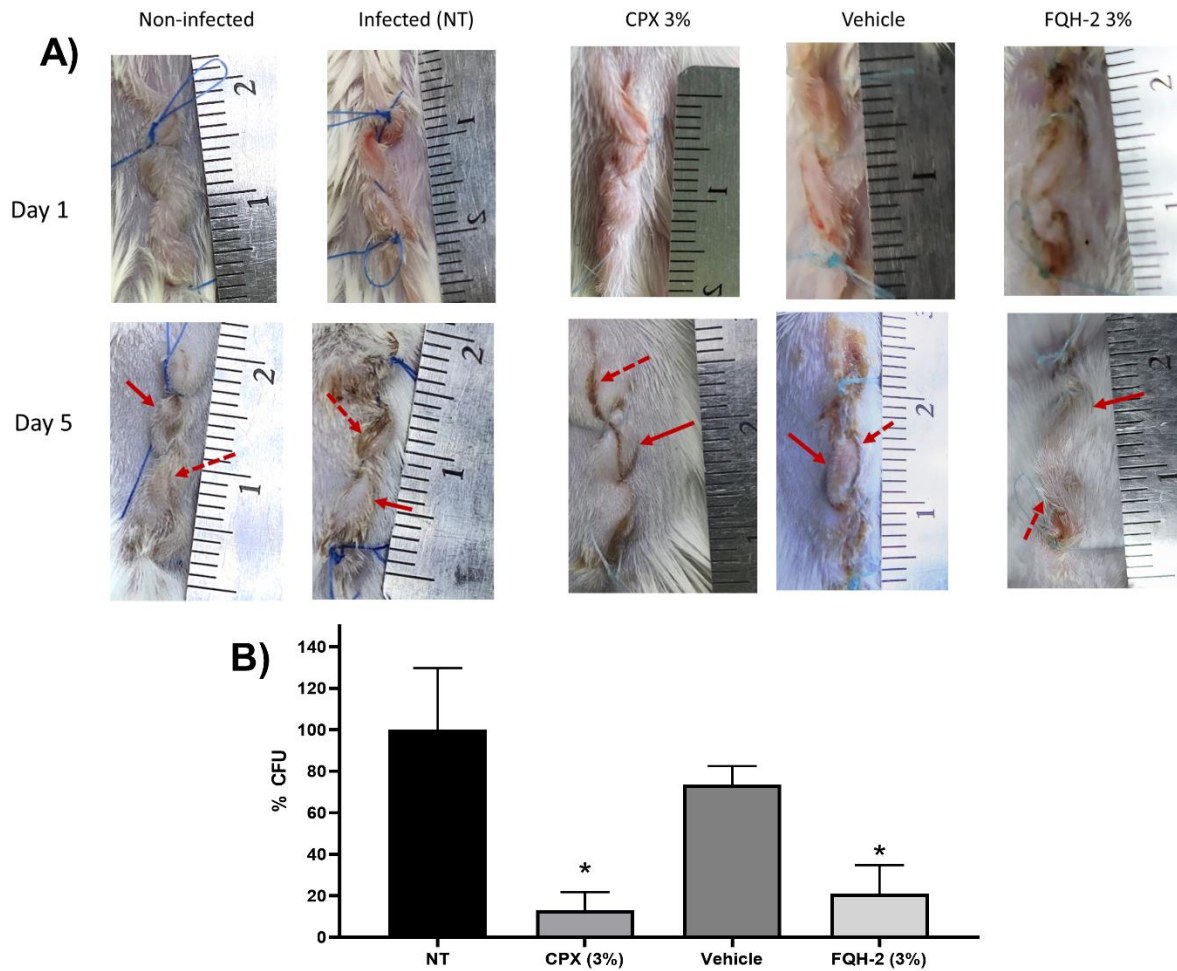


Figure 3. *In vivo* model of topical FQH-2 treatment and infection with *S. aureus* in mice.

In the column of the infected group (without treatment: NT), the pattern of contaminated wounds is demonstrated in the photographs from the 5th day, where the redness of the skin and edema are observed (continuous arrow). In addition, purulent secretions are perceived between the edges of the wound (dashed arrow), which causes the edges to be separated, generating a delay in healing due to *S aureus* infection. The subsequent columns are infected groups treated with **CPX** 3%, where the effect of the drug on the wound is observed, since there is no presence of pus, the edges of the skin are facing each other, and while a small amount of edema is present, there is no erythema. All of these factors can be interpreted as the normal course of healing. The column of the group infected and treated with the formulation of **FQH-2** has a behavior similar to the non-infected control, showing moderate inflammation and erythema, and apparent healing of the facing wound edges, unlike the group with the vehicle whose last image is more similar to the pattern of the NT group. At this point, the images show a reduction of

the infectious process with the administration of the **FQH-2**, however, it was necessary to confirm these results with the determination of the CFU's in the tissue of the contaminated wound.

In **Figure 3B**, the results for the amount of bacteria (% CFU) in the tissue of the infected wound are shown for each group (n=5). The control groups of NT and Vehicle had a similar bacterial burden, since they did not present significant differences, meaning that the hydric ointment has no effect on bacterial proliferation or inhibition ($P < 0.05$). However, the control group NT and the antimicrobial formulations of **CPX 3%** and **FQH-2** showed a marked decrease of CFU: $13.08\% \pm 19.52$ Vs 21.08 ± 27.38 respectively ($p < 0.05$). This data provide further evidence of the effective antimicrobial activity of **FQH-2**. Previous SAR studies on the antimicrobial activity of fluoroquinolones focus on studies *in vitro*, *in silico* or cytotoxic, however, a further level of evaluation was reached in this work with the *in vivo* model in mice. The infection was carried out with the *S. aureus* bacterium due to its clinical importance as the main etiologic agent in various infections, causing millions of serious infections worldwide [46], in addition to being a bacterium with constant mutations that generate antimicrobial resistance [47]. Therefore, future evaluations are needed on the pharmacodynamic and pharmacokinetic properties of **FQH-2** and its effects in tissues.

3. Conclusion

From SAR evaluation of fluoroquinolone analogues **FQH 1-5**, it was shown that fused aromatic heterocycles in position C-7 improve antimicrobial susceptibility in Gram-negative bacteria, and mainly in Gram-positive ones. The **FQH-2** compound (7-benzimidazole-1-yl-fluoroquinolone) was found to have the highest antimicrobial activity against *S. aureus*. In addition, during the antimicrobial evaluation using different experimental models, similar antimicrobial profiles and inhibitory activity among **FQH-2** and ciprofloxacin were observed. However, one advantage of **FQH-2** over the **CPX** is lower cytotoxicity against non-bacterial cells. For this reason, it was possible to show the antibiotic effect of **FQH-2** in the topical infection model in animals, where a decrease in CFU of *S. aureus* bacteria was detected which in turn contributed to the overall wound healing process. It is recommended that future research be directed towards the evaluation of resistant strains such as *S. aureus* to confirm its possible use against infections of strains with AMR and to further characterize the pharmacodynamic and pharmacokinetic properties of **FQH-2**.

4. Materials and methods

4.1 Reagents

Ciprofloxacin (Senosiain®), Dimethyl Sulfoxide DMSO (Sigma-Aldrich), Culture Medium as Nutrient Broth (BD Bioxon), Mannitol Salt Agar (BD Bioxon), Tryptic Soy Agar (Difco), Sodium Chloride (J.T. Baker), Triton x-100 (Sigma-aldrich), Sterile 9% Saline (AMSA Lab), Lymphoprep (STEMCELL), LIVE/DEAD™ Fixable Dead Cells Staining Kits (Invitrogen), RPMI (Gibco™), Sutures 4 zeros (American suture), sodium pentobarbital (Aranda Salud Animal), ciprofloxacin ointment “Sophixin” (Sophia).

4.2 Instrumentation

Melting points were obtained in a Fisher-Johns melting point apparatus. IR spectra were performed on a Thermo Nicolet iS10 spectrophotometer using the attenuated total reflectance (ATR) technique. Nuclear magnetic resonance (NMR) spectra were obtained on a Bruker Ascend 400MHz spectrophotometer.

4.3 Synthesis of fluoroquinolone analogues

In the **Figure 4** shows the synthesis of fluoroquinolone analogues with heterocycles at position C-7 on **FQH 1-5** was performed on the fluoroquinolone analogues **FQB-1** (7-(2,3,4,5-tetrahydro-carbazol-1-yl), **FQB-2** (7-benzimidazol-1-yl), **FQB-3** (7-uracil-1-yl), **FQB-4** (7-[5,5-diphenyl-hydantoin-1-yl]), and **FQB-5** (7-[3,5-diethoxycarbonyl-2,6-dimethyl-1,4-dihydropyridin-yl]), in the Organic Synthesis Laboratory of the Chemical Sciences Academic Unit of the Autonomous University of Zacatecas, Mexico, based on previous research focused on the synthesis of new fluoroquinolones with boron complexes [25].

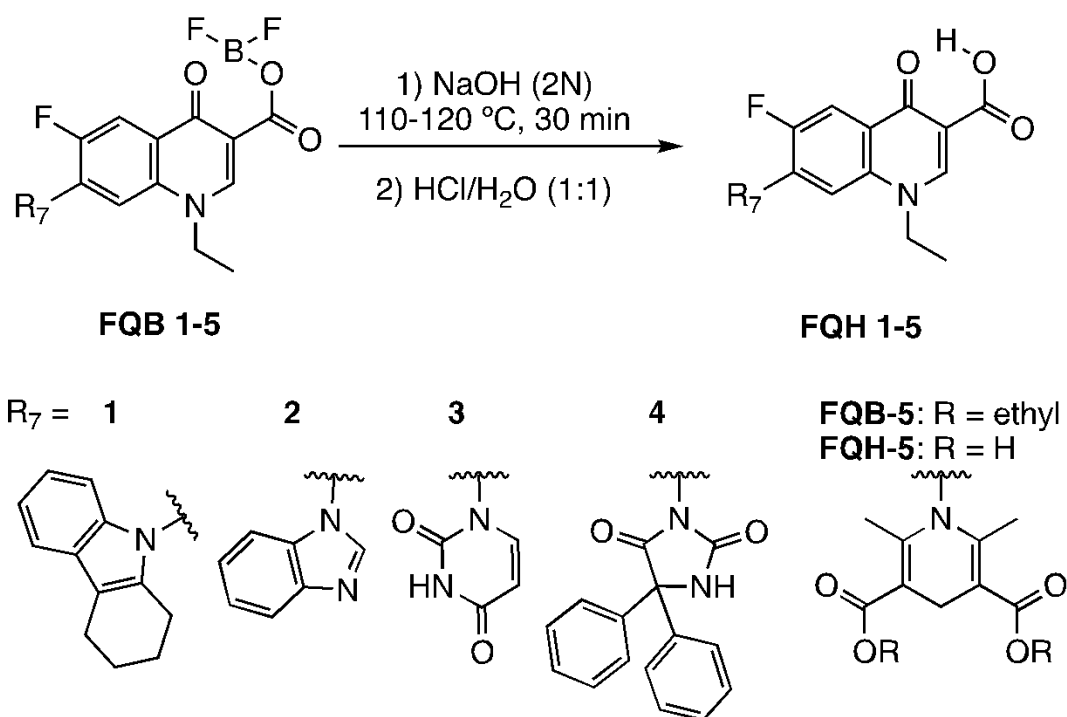


Figure 4. Synthesis of fluoroquinolone analogues FQH 1-5 by basic hydrolysis from fluoroquinolone-boron complexes FQB 1-5.

Subsequent hydrolysis of the boron complex in fluoroquinolones **FQB 1-5** in basic medium to obtain the fluoroquinolone 3-carboxylic acid molecules **FQH-1** (7-carbazol-1-yl), **FQH-2** (7-benzimidazole-1-yl), **FQH-3** (7-uracil-1-yl), **FQH-4** (7-[5,5-diphenyl-hydantoin-1-yl]), and **FQH-5** (7-[2,6-dimethyl-1,4-dihydropyridine-3,5-dicarboxylic acid]), was carried out as follows:

A round bottom flask was used with 100 mg of boron complex of the fluoroquinolone (221.2 μmol for **FQB-1**; 250.6 μmol for **FQB-2**; 254.4 μmol for **FQB-3**; 187.5 μmol for **FQB-4**; or 187.1 μmol for **FQB-5**), and an aqueous solution of 2N NaOH was added (792.6 μL for **FQB-1**; 898.2 μL for **FQB-2**; 911.9 μL for **FQB-3**; 672 μL for **FQB-4**; or 670 μL for **FQB-5**). The reaction mixture was refluxed for 30 minutes at a temperature of 110-120°C and after, slowly cooled to room temperature. An aqueous solution of HCl (1:1) v/v was then added dropwise until pH 7 was reached. A white solid was obtained which was vacuum filtered and washed with a neutral NaOH/HCl solution to remove excess NaOH. The corresponding 3-carboxylic acid-fluoroquinolone compounds **FQH 1-5** turned out with good yields. The **FQH 1-5** were dissolved in a 0.25N NaOH aqueous solution and stored at room temperature.

4.3.1 Chemical characterization of FQH 1-5

The molecule **FQH-1** (1-ethyl-7-(5*H*-1,2,3,4-tetrahydrocarbazole-5-yl)-6-fluoro-4-oxo-1,4-dihydroquinoline-3-carboxylic acid) is a white solid with a melting point (mp) of 318 °C and 73% (65.2mg) of reaction yield. The FTIR-ATR, ν (cm⁻¹): 3066-2946 (O—H, carboxylic acid), 1716 (C=O, carboxylic acid), 1616 (C=O, pyridone), 1561-1504 (C=C, aromatic), 1287-1212 (C—O, carboxylic acid), 1093 (C—F, aromatic).

The 1-ethyl-7-(1*H*-benzimidazole-1-yl)-6-fluoro-4-oxo-1,4-dihydroquinoline-3-carboxylic acid labeled as **FQH-2** is a white solid with mp 330°C and 90% (79.2mg) reaction yield. FTIR-ATR, ν (cm⁻¹): 3208-2983 (O—H, carboxylic acid), 1704 (C=O, carboxylic acid), 1613 (C=O, pyridone), 1582-1542 (C=C, aromatic), 1299-1088 (C—O, carboxylic acid), 1036 (C—F, aromatic).

The 1-ethyl-6-fluoro-4-oxo-7-(uracil-1-yl)-1,4-dihydroquinoline-3-carboxylic acid labeled **FQH-3** is a white solid with mp of 311 °C and 59% (51.8 mg) of reaction yield. The FTIR-ATR, ν (cm⁻¹) 3062-2926 (O—H, carboxylic acid), 1697 (C=O, carboxylic acid), 1615 (C=O, pyridone), 1558-1473 (C=C, aromatic), 1287-1229 (C—O, carboxylic acid), 1042 (C—F, aromatic).

The 1-ethyl-6-fluoro-7-(5,5-diphenylhydantoin-3-yl)-4-oxo-1,4-dihydroquinoline-3-carboxylic acid labeled as **FQH-4** is a white solid with mp of 297 °C and 66% (60.1mg) of reaction yield. FTIR-ATR, ν (cm⁻¹): 3065-2948 (O—H, carboxylic acid), 1716 (C=O, carboxylic acid), 1616 (C=O, pyridone), 1560-1484 (C=C, aromatic), 1306-1093 (C—O, carboxylic acid), 1041 (C—F, aromatic).

The 1-(3-carboxy-1-ethyl-6-fluoro-4-oxo-1,4-dihydroquinolin-7-yl)-2,6-dimethyl-1,4-dihydropyridine-3,5-dicarboxylic acid labeled as **FQH-5** is a white solid with mp 309 °C and 50% (40.0 mg) reaction yield. FTIR-ATR, ν (cm⁻¹): 3066 -2961 (O—H, carboxylic acid), 1716 (C=O, carboxylic acid), 1616 (C=O, pyridone), 1561 (C=C, aromatic) , 1213-1288 (C—O, carboxylic acid), 1042-1093 (C—F, aromatic).

4.4 Antimicrobial activity

Bacterial strains. Four bacterial strains were evaluated *in vitro*, where two of them were the Gram-positive microorganisms *S. aureus* (ATCC 23235™) and *E. faecalis* (ATCC 29212™), and the other two were the Gram-negative *E. coli* (ATCC 25922™) and a strain of *K. pneumoniae* of a clinical isolate sensitive to ciprofloxacin. For the *in vivo* evaluation, a strain of *S. aureus* from a clinical isolate sensitive to ciprofloxacin and **FQH 1-5** was used. Both types of clinical isolates were obtained from the strain collection of the Experimental Immunotoxicology and Therapeutics Laboratory of the Academic Unit of Chemical Sciences at the Autonomous University of Zacatecas, Mexico.

4.5 *In vitro* antimicrobial activity assays for the determination of the Minimum Inhibitory Concentration (MIC) and Minimum Bactericidal Concentration (MBC)

The review of the antibacterial activity of the compounds **FQH 1-5** was performed using the microdilution method in standardized broth, in accordance with the method reported by the Clinical and Laboratory Standards Institute (CLSI) M07 11th edition M100 30th [48, 49]. The evaluation of the Minimum Inhibitory Concentration (MIC) was carried out through microdilution in 96-well plates, with 1.5×10^5 CFU/mL of each of the bacteria mentioned in the previous section. Each one was exposed to a range of serial dilution concentrations according to the standardized values in the MIC break points of ciprofloxacin (CPX), specific for each bacterial strain, which also functioned as reference control. **FQH 1-5** compounds were treated similarly with their respective concentrations for each bacterium. The same dilution conditions were used for the vehicle control, which consisted of an aqueous solution. All 96-well plates with the different conditions (**FQH 1-5**, CPX and the vehicle) were incubated at 37 °C for 24 h until the experimental inhibitory concentration (breakpoint), which was determined when no turbidity was observed at the bottom of the well after 24 h of incubation.

The Minimum Bactericidal Concentration (MBC) was determined by taking samples from the wells close to the MIC for each bacterial strain to later reseed them in Petri dishes with trypticase soy agar and incubate them for 24 h at 37 °C. The value of MBC was established from the areas where the development of colony-forming units (CFU) was not shown. All assays were carried out in triplicate for all bacterial strains and the **FQH 1-5** [50].

4.6 Molecular docking

The *in silico* model was carried out by means of three crystallized proteins of DNA Topoisomerase II (Topo II), downloaded from the Protein Data Bank (PDB) database shown in **table 2**. These proteins have a co-crystallized fluoroquinolone in the active site [51]. The chemical structures of the **FQH 1-5** were drawn in the Marvin Sketch program (Marvin version 21.17.0, ChemAxon <https://www.chemaxon.com>). The proteins were edited to obtain the receptor and ligand in the USCF Chimera program [52]. The coupling of the ligand for each receptor in its respective bacterial was carried out through the Autodock-vina program which uses the Lamarckian Genetic Algorithm (LGA) and is based on semi-empirical free energy fields. In the Autodock program, tools were used to identify the coordinates and sizes of the grid box to dock the **FQH 1-5**, based on the location of the co-crystallized ligand. Results are shown from the binding energy score as the ligand pose was retained for analysis. Co-crystallized ligand docking scores were taken as the reference values [53] (used to compare the

results of docked FQHs). All the proteins had the same treatment, with the exception of that of *E. coli* (6rkv). Due to its characteristics, a different molecular strategy was used, since it was done through blind docking [54], where the complete structure of the protein was taken as the pocket (grid box), and sites of interaction were confirmed using the Protein Plus server [55]. In addition, interactions in this model were evaluated with the Pymol program [56]. For a better understanding of the binding energy scores, analysis was done through a heat map using the Heat mapper server [57].

Table 1. Protein Characteristics					
Strain	PDB code	DNA topoisomerase IIA	Resolution (Å)	Adjunct Molecules	Reference
<i>Klebsiella pneumoniae</i>	5eix	DNA Topoisomerases IV	3.35	Magnesium Levofloxacin	[58]
<i>Staphylococcus aureus</i>	5cdq	DNA Gyrase	2.95	Glycerol Magnesium Moxifloxacin	[59]
<i>Escherichia coli</i>	6 rkv	DNA Gyrase	4.60	----	[60]

4.7 Cytotoxicity assays

Venous blood obtained from healthy volunteers in EDTA tubes was diluted 1:1 with RPMI medium, and carried with Lymphoprep™ in a 15ml propylene conical tube [61]. After centrifugation (800g, 30 min), peripheral blood mononuclear cells (PBMCs) were seeded and stored in a conical tube with fresh RPMI medium and cells were washed three times with phosphate buffered saline (450g, 5 min). Finally, the PBMC were resuspended in RPMI medium supplemented with 10% Fetal Bovine Serum (FBS) and cell number and viability (>95%) were determined. Next, 500,000 cells per well were seeded in a 12-well plate and the cells were exposed to different conditions [62]: without stimulation (viability control), at a concentration of 4.39µm of Dimethyl Sulfoxide (DMSO) as positive control, toxic concentrations of ciprofloxacin 500 µg/ml (reference control), aqueous solution of H₂O/NaOH (vehicle control) and increasing concentrations of the selected **FQH 1-5**. Cells were incubated at 36 °C for 24 h with 5% CO₂. Afterwards, cells in suspension were collected and transferred to polystyrene round-bottom tubes and washed twice with PBS. Cell staining is then done using the LIVE/DED™ Fixable Dead Cell Stain Kit dye (Invitrogen, USA), following the manufacturer's instructions. Finally, all the samples were measured in a FACS CANTO II flow cytometer with a 4-2-2 configuration (BectonDickson, USA), and analyzed with the FlowJo v 10.0 program (BD, Bioscience, USA).

4.8 Evaluation of the antimicrobial activity of FQH-2 in an *in vivo* model of topical infection

Animals. Pathogen-free BALB/c mice with a weight range between 25-30 g were used in all experiments, purchased from a commercial source (Centro de Biociencias de la Universidad Autónoma de San Luis Potosí, San Luis Potosí, México). The animals were cared for in the Bioterio “*Claude Bernard*” in the Area of Health Sciences of the Autonomous University of Zacatecas, Zacatecas, Mexico. They were kept in individual boxes at a temperature of 22-24 °C with controlled humidity, and were allowed food and water *ad libitum* [63]. The animals were divided into five groups (n=5): a group without infection (non-infected), which were mice with surgical wounds without infectious agent. Groups of mice with *S. aureus* infected wounds were treated as follows: no treatment (NT) group, 3% Ciprofloxacin (**CPX**) (Sophixin™ ointment) group, vehicle group (aqueous solution ointment) and previously prepared 3% **FQH-2** ointment administration group.

Ointment preparation. A **FQH-2** ointment was prepared from a hydrophilic base: 50 mg of carbapol were completely dissolved in 10 ml of a solution of sterile distilled water and 3% **FQH-2**. 1 ml of triethanolamine was then added with constant stirring until consistency changed to colloid. Finally, 3% **FQH-2** ointment (prepared from a premade 5 mg/mL solution) was stored at room temperature [64].

In vivo model of topical infection. The antimicrobial effect of the **FQH-2** was evaluated according to the McRipley and Within protocol, making some material adaptations. In this topical infection model, suture contamination was performed with a strain of *S. aureus* (sensitive to ciprofloxacin). To do this, an inoculum of *S. aureus* 2×10^9 CFU/mL in a 0.85% NaCl solution was prepared in which sterile medical sutures (11 cm) were added for 30 min, and were then dried on a sterile surface [65-68]. Mice were anesthetized with 75 mg/kg pentobarbital and topical lidocaine [69]. The lesion area was sterilized with aseptic solutions and surgery was performed on the back of the shaved animals, by means of a 2 cm longitudinal cut in the downward direction of the meaty panniculus under sterile conditions [68]. At the end of the procedure, the recovery of the animals was monitored. The infectious process was followed for five days. After this, the animals were sacrificed according to NOM-033-ZOO-1995 with CO₂ in a pathogen-free environment. Wound tissue (uninfected and infected) was collected and processed for bacterial count which was done on the maceration of the tissue with a sterile solution of NaCl 0.85%. A serial dilution was then carried out. To take a sample of each one of the dilutions and sow them in Petri dishes with salt and mannitol agar, they were incubated for 24 h at 37 °C. After this time, the colonies were counted (CFU/mL) in order to gather all the data of the results for their analysis and interpretation [64-66, 68].

Dosage. The administrations were 500 mg of ointment in each animal, starting at 5 h post-surgery, with subsequent dosages carried out every 12 h until day 5. The application of each of the formulations was done with a metal spatula (previously sterilized) and in an aseptic environment.

This methodology was approved by the Bioethics Committee of the Health Sciences Area of the Autonomous University of Zacatecas, with registration number ACS/UAZ182/2022. All procedures were performed in accordance with NOM-062-Z00-199, as well as under consideration of international guidelines for choosing a correct end point in research with experimental animals [63, 67].

4.9 Statistical analysis

The data from the experimental results was analyzed in the Graph Pad Prism version 8.0 program. Normality tests were performed to later apply multiple comparison tests between the groups using the one-way ANOVA test with Tukey's post-test. Significant difference values were considered from * $p < 0.05$ to **** $p < 0.0001$ in all analyses.

Supplementary Materials: Not applicable

Acknowledgments: The author (M.F. Medellín-Luna) acknowledges CONCYT for the economic support during the realization this investigation with scholarship number **733912** Also, the methodology support of Fuensanta Reyes Escobedo PhD of Microbiology Lab of Academic Unit of Chemical Sciences of the Autonomous University of Zacatecas.

Author Contributions: Conceptualization: A.R.C.V, H.H.L and J.E.C.D; methodology: chemistry: M.F.M.L H.H.L, microbiology: M.F.M.L F. M.G, molecular docking: E.L.R, cytotoxic: M.F.M.L J.E.C.D, animal model: S.G.C and J.J.E.R; investigation: M.F.M.L; writing-original draft preparation: M.F.M.L and H.H.L; writing –reviewed and editing: M.F.M.L, H.H.L J.E.C.D. and A.R.C.V; visualization: M.F.M.L; supervision: D.P.P, A.R.C.V. All authors have read and agreed to publisher version of manuscript

Founding: This research received no external funding

Institutional Reviewed Board Statement: The *in vivo* model of topical infection was approved for Bioethics Committee of the Health Sciences Area of the Autonomous University of Zacatecas with registration number ACS/UAZ/182/2022, also all procedures were performed in accordance with NOM-062-ZOO-199 and it was considered an international guideline for choosing an appropriate end point in animal experiments for research, teaching, and experimentation of *Canadian Council on Animal Care*. Euthanasia was in accordance with the NOM-033-ZOO-1995. Currently regulation to management and care of experimental animals in Mexico.

Informed Consent Statement: Not applicable

Data Availability Statement: Not applicable

Conflicts of Interest: The authors declare no conflicts of interest

Sample Availability: Not applicable

Figure Legends

Figure 1. Molecular docking analysis of FQH-2 with Topoisomerase II from several bacterial strains. Molecular docking was done in a downloaded protein of PDB: *E. coli* (6 rkv), *S. aureus* (5cdq), and *K. pneumoniae* (5eix), which included a co-crystallized fluoroquinolone, as well as a DNA and magnesium ion; the preparation of molecules was performed in the same way, except for the protein *E. coli* in which all protein was taken as the pocket to direct the ligands and found of inhibition allosteric sites and check the site to use to the binding pocket. The docking process was done with the program Autodock vina. The results were scored on binding energies analyzed in a heatmap and the docked ligands were reviewed in the Pymol program. **A)** Displays a heatmap on scores of binding energy, in each cell represents a score of FQH 1-5 with Topo II, respectively. The colors indicate the strength of binding energies, where red represents lower energy (kcal/mol) and blue represents higher binding energy, the compounds with lower score predict higher binding and therefore a plausible biological effect. The FQH-2 had lower scores for both bacterial strains (Gram-positive and –negative). Therefore, it was selected for further analysis on the orientation and binding pose. **B)** We show the interactions in the binding pocket through of topological area surface, in orange color shows the contacts of FQH-2 with key amino acids of protein. **C)** This picture shows the overlapping of moxifloxacin (cyan color) and FQH-2 (red color) in the target.

Figure 2. Non-cytotoxic effect of FQH-2 in peripheral blood mononuclear cells. PBMC's were extracted with lymphoprep and seeded to 500,000 cells per well in a 12-well plate. non-treated (FBS 10%, also for all other conditions), positive (DMSO, 4.39 μ M), CPX (ciprofloxacin, 500 mg/ml), vehicle (aqueous solution of H₂O/NaOH) and increasing concentrations of 128-4mg/ml of FQH-2. After 24h of incubations, the cells were stained with kit Live/Dead staining reagent (Invitrogen), lastly, each condition was acquired for flow cytometry; the data were analyzed in the FlowJo software. **A)** We display the populations in a stacked histogram for each condition, the fluorescence increment (side right of x axes) represent death population of cell, then opposite are viable population. **B)** Percent mortality is shown based on flow cytometry data. No significant differences among FQH-2 concentrations were observed. The graph shows the mean standard deviation of three independent experiments. A One-way ANOVA statistical test with a Tukey post-hoc was performed with ****p<0.0001

Figure 3. In vivo model of topical FQH-2 treatment and infection with *S. aureus* in mice. BALB/c mice were divided into five groups (n=5): Non-infected (NT), Infected, Commercial ciprofloxacin ointment 3% (CPX 3%), Vehicle (aqueous gel-based solution), and FQH-2 (formulation of FQH-2 in gel). Surgery and wound infection were performed on the animals according to the McRipley protocol, for the groups CPX, Vehicle, and FQH-2 were administered 5 h post-surgical and photographic documentation of the wounds was performed throughout the experiment. On day 5 the animals were sacrificed and the tissues were collected and processed for CFU counts. **A)** Representative images of a mouse for each group; the lines represent day 1 (surgery) and day 5 (end tracking), and the columns show the conditions. The arrows presented in the images refer to the main characteristics of wound infection, like inflammation (continue arrow $\}$) and wound edge swelling (discontinuous arrow \uparrow) **B)** CFU counts were analyzed wound tissues according to the infectious group. The comparison is made between the groups infected with treatment, hence, the CPX and FQH-2 had significant differences from the SE (infection) group, although the FQH-2 had a higher percentage than CPX. The graph shows the mean and standard deviation, statistical test of ANOVA one-way with post-test of Tukey *p<0.05, **p<0.01, ***p<0.0001.

Figure 4. Synthesis of fluoroquinolone analogues FQH 1-5 by basic hydrolysis from fluoroquinolone-boron complexes FQB 1-5.

References

1. *Antibacterial agents in clinical and preclinical development: an overview and analysis*. Geneva. 2022, World Health Organization.
2. Organization, W.H. *Antimicrobial resistance*. (2018); Available from: <https://apps.who.int/iris/handle/10665/255204>.
3. Organization, W.H., *Global action plan on antimicrobial resistance*, W.H. Organization, Editor. 2015: Geneva.
4. Organization, W.H., *WHO publishes list of bacteria for which new antibiotics are urgently needed*. 2017.
5. Ikuta, K.S., et al., *Global mortality associated with 33 bacterial pathogens in 2019: a systematic analysis for the Global Burden of Disease Study 2019*. The Lancet.
6. Theuretzbacher, U., et al., *The global preclinical antibacterial pipeline*. Nat Rev Microbiol, 2020. **18**(5): p. 275-285.
7. Kaur, R., et al., *Discovery and Development of Antibacterial Agents: Fortuitous and Designed*. Mini Rev Med Chem, 2022. **22**(7): p. 984-1029.
8. Tacconelli, E., et al., *Discovery, research, and development of new antibiotics: the WHO priority list of antibiotic-resistant bacteria and tuberculosis*. Lancet Infect Dis, 2018. **18**(3): p. 318-327.
9. Reguero, M.T., E. Barreto, and F.J.R.C.d.C.Q.-F. Jiménez, *Relación estructura química actividad biológica: una revisión retrospectiva*. 1989. **17**(1): p. 81-84.
10. Lin, H., *The Computational Methods in Drug Targets Discovery*. Curr Drug Targets, 2019. **20**(5): p. 479-480.
11. Tutone, M. and A.M. Almerico, *Computational Approaches: Drug Discovery and Design in Medicinal Chemistry and Bioinformatics*. Molecules, 2021. **26**(24).
12. Fedorowicz, J. and J. Sączewski, *Modifications of quinolones and fluoroquinolones: hybrid compounds and dual-action molecules*. Monatsh Chem, 2018. **149**(7): p. 1199-1245.
13. Takahashi, H., I. Hayakawa, and T. Akimoto, *[The history of the development and changes of quinolone antibacterial agents]*. Yakushigaku Zasshi, 2003. **38**(2): p. 161-79.
14. Ball, P., *Chapter 1 - The Quinolones: History and Overview*, in *The Quinolones (Third Edition)*, V.T. Andriole, Editor. 2000, Academic Press: San Diego. p. 1-31.
15. Pham, T.D.M., Z.M. Ziora, and M.A.T. Blaskovich, *Quinolone antibiotics*. MedChemComm, 2019. **10**(10): p. 1719-1739.
16. Madurga, S., et al., *Mechanism of binding of fluoroquinolones to the quinolone resistance-determining region of DNA gyrase: towards an understanding of the molecular basis of quinolone resistance*. Chembiochem, 2008. **9**(13): p. 2081-6.
17. Wolfson, J.S. and D.C. Hooper, *The fluoroquinolones: structures, mechanisms of action and resistance, and spectra of activity in vitro*. Antimicrob Agents Chemother, 1985. **28**(4): p. 581-6.
18. Pham, T.D.M., *Quinolone antibiotics*, in *Research, T.s.-a.r.S.o. quinolones*, Editor. 2019.
19. Peterson, L.R., *Quinolone Molecular Structure-Activity Relationships: What We Have Learned about Improving Antimicrobial Activity*. Clinical Infectious Diseases, 2001. **33**(Supplement_3): p. S180-S186.
20. Maxweell. A, C.S.E., *Mode of Action*, in *Quinolone Antibacterials*, D.A.a.Z.H.-J. Kuhlmann. J, Editor. 1998: Germany.
21. Bax, B.D., et al., *Type IIA topoisomerase inhibition by a new class of antibacterial agents*. Nature, 2010. **466**(7309): p. 935-40.
22. Azam, M.A., J. Thathan, and S. Jubie, *Dual targeting DNA gyrase B (GyrB) and topoisomerase IV (ParE) inhibitors: A review*. Bioorganic Chemistry, 2015. **62**: p. 41-63.
23. Bush, N.G., K. Evans-Roberts, and A. Maxwell, *DNA Topoisomerases*. EcoSal Plus, 2015. **6**(2).
24. Higgins, P.G., A.C. Fluit, and F.J. Schmitz, *Fluoroquinolones: structure and target sites*. Curr Drug Targets, 2003. **4**(2): p. 181-90.

25. Hernández-López, H., et al., *Synthesis of Hybrid Fluoroquinolone-Boron Complexes and Their Evaluation in Cervical Cancer Cell Lines*. Journal of Chemistry, 2019. **2019**: p. 5608652.
26. Chu, D., P.B.J.A.a. Fernandes, and chemotherapy, *Structure-activity relationships of the fluoroquinolones*. 1989. **33**(2): p. 131-135.
27. Wang, Y.N., et al., *Discovery of Benzimidazole-Quinolone Hybrids as New Cleaving Agents toward Drug-Resistant Pseudomonas aeruginosa DNA*. ChemMedChem, 2018. **13**(10): p. 1004-1017.
28. Kitchen, D.B., et al., *Docking and scoring in virtual screening for drug discovery: methods and applications*. Nat Rev Drug Discov, 2004. **3**(11): p. 935-49.
29. Pintilie, L.S., A. , *Molecular Docking Studies of Some Novel Fluoroquinolone Derivatives.*, in *Preprints* 2019.
30. Lucia, P., et al., *Design, Synthesis and Docking Studies of Some Novel Fluoroquinolone Compounds with Antibacterial Activity*. Revista de Chimie -Bucharest- Original Edition-, 2018. **69**.
31. Allaka, T.R., et al., *Molecular Modeling Studies of Novel Fluoroquinolone Molecules*. Curr Drug Discov Technol, 2018. **15**(2): p. 109-122.
32. Millanao, A.R., et al., *Biological Effects of Quinolones: A Family of Broad-Spectrum Antimicrobial Agents*. Molecules, 2021. **26**(23).
33. Salahuddin, M. Shaharyar, and A. Mazumder, *Benzimidazoles: A biologically active compounds*. Arabian Journal of Chemistry, 2017. **10**: p. S157-S173.
34. Bansal, Y., M. Kaur, and G. Bansal, *Antimicrobial Potential of Benzimidazole Derived Molecules*. Mini Rev Med Chem, 2019. **19**(8): p. 624-646.
35. Akhtar, M.J., et al., *Recent Progress of Benzimidazole Hybrids for Anticancer Potential*. Curr Med Chem, 2020. **27**(35): p. 5970-6014.
36. Pandey, V. and A. Shukla, *Synthesis and biological activity of isoquinoliny benzimidazoles*. 1999.
37. Küçükbay, H., et al., *Synthesis of some benzimidazole derivatives and their antibacterial and antifungal activities*. Arzneimittelforschung, 2001. **51**(5): p. 420-4.
38. Tülay Aşkin, Ç., *Introductory Chapter: Cytotoxicity*, in *Cytotoxicity*, Ç. Tülay Aşkin, Editor. 2018, IntechOpen: Rijeka. p. Ch. 1.
39. Azéma, J., et al., *7-((4-Substituted)piperazin-1-yl) derivatives of ciprofloxacin: synthesis and in vitro biological evaluation as potential antitumor agents*. Bioorg Med Chem, 2009. **17**(15): p. 5396-407.
40. Duwelhenke, N., O. Krut, and P. Eysel, *Influence on mitochondria and cytotoxicity of different antibiotics administered in high concentrations on primary human osteoblasts and cell lines*. Antimicrob Agents Chemother, 2007. **51**(1): p. 54-63.
41. Kloskowski, T., et al., *Ciprofloxacin is a potential topoisomerase II inhibitor for the treatment of NSCLC*. Int J Oncol, 2012. **41**(6): p. 1943-9.
42. Cheung, G.Y.C., J.S. Bae, and M. Otto, *Pathogenicity and virulence of Staphylococcus aureus*. Virulence, 2021. **12**(1): p. 547-569.
43. Johnson, M.K., *Impetigo*. Adv Emerg Nurs J, 2020. **42**(4): p. 262-269.
44. Tapia, A.G.P., et al., *Prevalencia de infección de herida quirúrgica, causas y resistencia a los fármacos en el Hospital General de Zona núm. 2 del IMSS, San Luis Potosí*. 2012. **17**(4): p. 261-265.
45. Kamel C, M.L., Mierzwinski-Urban M, et al. , *Appendix 1. Classification of surgical wounds*, in *Preoperative Skin Antiseptic Preparations and Applications Techniques for Preventing Surgical Site Infections: A systematic Review of the clinical evidence and guidelines*, Internet, Editor. 2011 Jun, Canadian Agency for Drugs and Technologies in Health: Ottawa (ON).
46. Lakhundi, S. and K. Zhang, *Methicillin-Resistant Staphylococcus aureus: Molecular Characterization, Evolution, and Epidemiology*. Clin Microbiol Rev, 2018. **31**(4).
47. Rasigade, J.P., O. Dumitrescu, and G. Lina, *New epidemiology of Staphylococcus aureus infections*. Clin Microbiol Infect, 2014. **20**(7): p. 587-8.

48. Wikler, M.A.J.C., *Methods for dilution antimicrobial susceptibility tests for bacteria that grow aerobically: approved standard*. 2006. **26**: p. M7-A7.
49. CLSI, *Performance Standards for Antimicrobial Susceptibility Testing*. 2022, Clinical and Laboratory Standards Institute.
50. Clinical and L.S.I.J.C.s. M100, *Performance standards for antimicrobial susceptibility testing*. 2017, Clinical and Laboratory Standards Institute Wayne, PA.
51. Agrawal, P., et al., *Benchmarking of different molecular docking methods for protein-peptide docking*. BMC Bioinformatics, 2019. **19**(Suppl 13): p. 426.
52. Pettersen, E.F., et al., *UCSF Chimera—A visualization system for exploratory research and analysis*. 2004. **25**(13): p. 1605-1612.
53. Trott, O. and A.J. Olson, *AutoDock Vina: improving the speed and accuracy of docking with a new scoring function, efficient optimization, and multithreading*. J Comput Chem, 2010. **31**(2): p. 455-61.
54. Morris, G.M. and M. Lim-Wilby, *Molecular Docking*, in *Molecular Modeling of Proteins*, A. Kukol, Editor. 2008, Humana Press: Totowa, NJ. p. 365-382.
55. Fährrolfes, R., et al., *ProteinsPlus: a web portal for structure analysis of macromolecules*. Nucleic Acids Res, 2017. **45**(W1): p. W337-w343.
56. Schrödinger, L., *The PyMOL Molecular Graphics System*.
57. Babicki, S., et al., *Heatmapper: web-enabled heat mapping for all*. Nucleic Acids Res, 2016. **44**(W1): p. W147-53.
58. Veselkov, D.A., et al., *Structure of a quinolone-stabilized cleavage complex of topoisomerase IV from Klebsiella pneumoniae and comparison with a related Streptococcus pneumoniae complex*. Acta Crystallogr D Struct Biol, 2016. **72**(Pt 4): p. 488-96.
59. Chan, P.F., et al., *Structural basis of DNA gyrase inhibition by antibacterial QPT-1, anticancer drug etoposide and moxifloxacin*. Nat Commun, 2015. **6**: p. 10048.
60. Vanden Broeck, A., et al., *Cryo-EM structure of the complete E. coli DNA gyrase nucleoprotein complex*. Nat Commun, 2019. **10**(1): p. 4935.
61. Grievink, H.W., et al., *Comparison of Three Isolation Techniques for Human Peripheral Blood Mononuclear Cells: Cell Recovery and Viability, Population Composition, and Cell Functionality*. Biopreserv Biobank, 2016. **14**(5): p. 410-415.
62. Fernández-Ruiz, J.C., et al., *GPR15 expressed in T lymphocytes from RA patients is involved in leukocyte chemotaxis to the synovium*. J Leukoc Biol, 2022.
63. Council, N.R., *Guide for the care and use of laboratory animals*. 2010.
64. Bele, A.A., et al., *Antibacterial potential of herbal formulation*. 2009. **4**(4): p. 164-167.
65. Rittenhouse, S., et al., *Use of the surgical wound infection model to determine the efficacious dosing regimen of retapamulin, a novel topical antibiotic*. Antimicrob Agents Chemother, 2006. **50**(11): p. 3886-8.
66. Petsch JD, J.P.H., *Murine Thigh Suture Model*, in *Handbook of Animals Models of Infection: Experimental Models in Antimicrobial Chemotherapy*, S.M. Zak O, Editor. 1999, Academic Press: USA.
67. Morton, D.B. and P.H. Griffiths, *Guidelines on the recognition of pain, distress and discomfort in experimental animals and an hypothesis for assessment*. Vet Rec, 1985. **116**(16): p. 431-6.
68. McRipley, R.J. and R.R. Whitney, *Characterization and quantitation of experimental surgical-wound infections used to evaluate topical antibacterial agents*. Antimicrob Agents Chemother, 1976. **10**(1): p. 38-44.
69. Soma, L.R.J.A.o.t.N.Y.A.o.S., *Anesthetic and analgesic considerations in the experimental animal*. 1983.

Anexos

Supplementary Information

Fluoroquinolone Analogues SAR Analysis and the Antimicrobial Evaluation of 7-Benzimidazol-1-yl-fluoroquinolone in *In Vitro*, *In Silico*, and *In Vivo* Models

Mitzzy Fátima Medellín-Luna^{1,2,3}, Hiram Hernández-López², Julio Enrique Castañeda-Delgado^{3,4}, Fidel Martínez- Gutierrez¹, Edgar Lara-Ramírez^{3,5}, Joan Jair Espinoza Rodríguez², Salvador García- Cruz⁴, Diana Patricia Portales-Pérez¹, Alberto Rafael Cervantes-Villagrana^{2,*}

¹ Doctorado en Ciencias Farmacobiológicas, Facultad de Ciencias Químicas, Universidad Autónoma de San Luís Potosí, 78210 San Luis Potosí, México.

² Unidad Académica de Ciencias Químicas, Universidad Autónoma de Zacatecas, 98160, Zacatecas, México.

³ Unidad de Investigación Biomédica de Zacatecas, Instituto Mexicano del Seguro Social, 98000, Zacatecas, México.

⁴ Investigadores por México, CONAHCYT, Consejo Nacional de Humanidades, ciencias y tecnologías, 03940 Ciudad de México, México.

⁵ Laboratorio de Biotecnología Farmacéutica, Centro de Biotecnología Genómica, Instituto Politécnico Nacional, 88710 Reynosa, Tamaulipas, México.

⁶ Departamento de Cirugía experimental e Investigación Quirúrgica y Bioterio. "Claude Bernard". Área de Ciencias de la Salud. Universidad Autónoma de Zacatecas, 98160, Zacatecas, México;

* Author of Correspondence: dr.albertocervantes@uaz.edu.mx

Content

Binding energy score for docking calculations.....	S35
FTIR – ATR spectra	S36
NMR spectra.....	S38
Thin Layer Chromatography	S39

Binding energy score for docking calculations

Bacterial	Reference Ligand (kcal/mol)	FQH-1 (kcal/mol)	FQH-2 (kcal/mol)	FQH-3 (kcal/mol)	FQH-4 (kcal/mol)	FQH-5 (kcal/mol)
<i>S. aureus</i> (5cdq)	-11.30	-10.9	-10.6	-10.4	-8	-8.4
<i>E. coli</i> (6rkv)	-11.3	-10.9	-9.9	-9.2	-7.8	-8.9
<i>K. pneumonia</i> (5eix)	-10.6	-7	-9.1	-9.7	8.8	-7.1

FTIR – ATR spectra

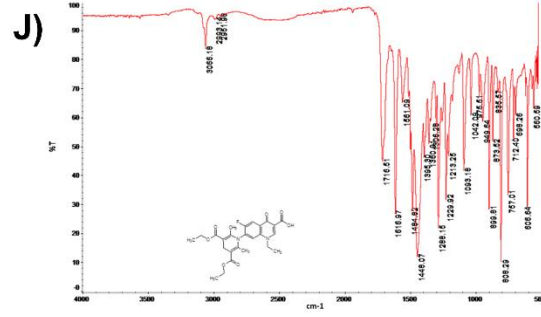
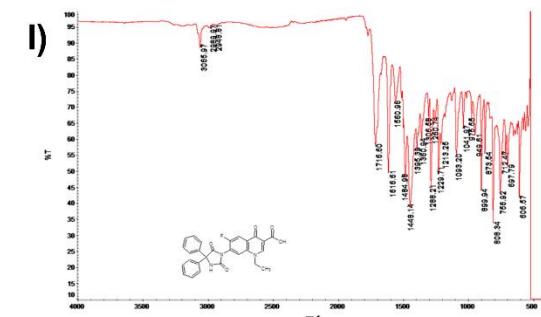
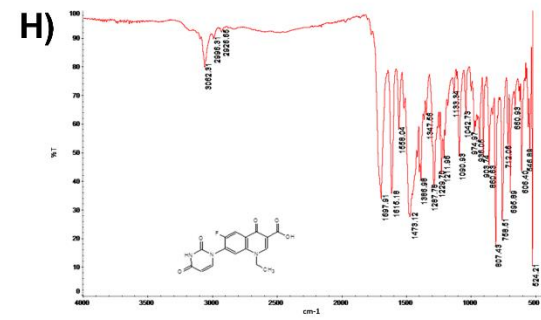
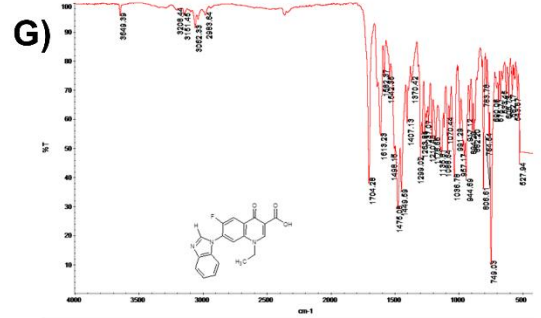
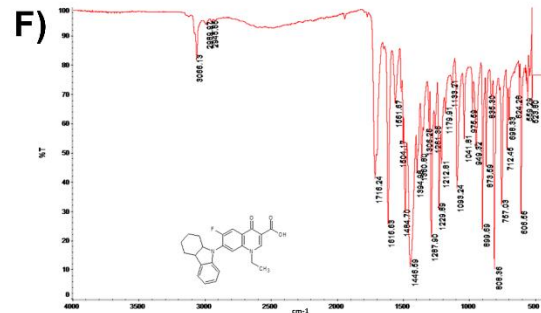
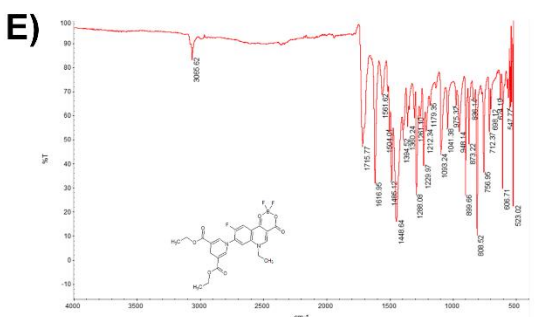
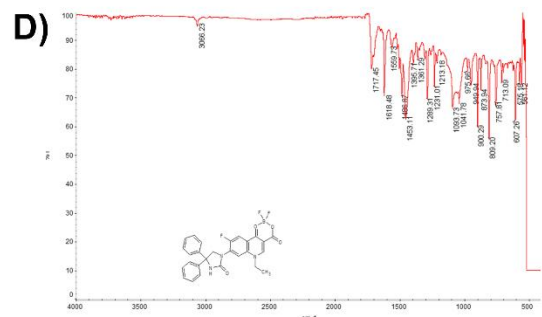
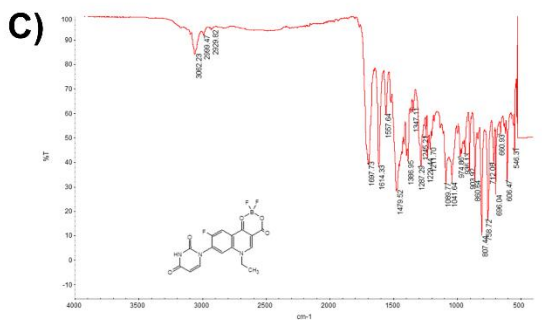
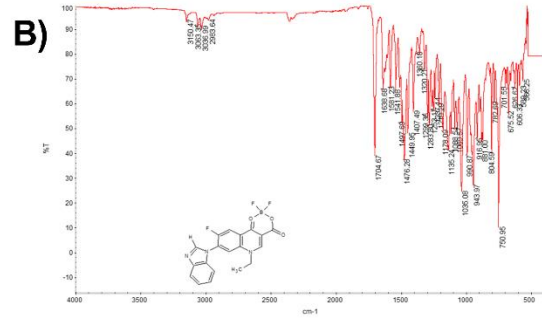
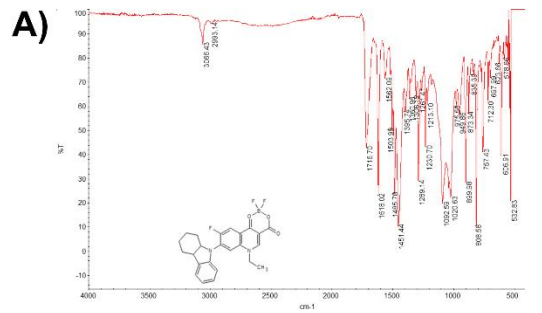


Figure S1. FTIR-ATR spectra of fluoroquinolone analogues FQB 1-5 and FQH 1-5. **A)** Difluoroboranyl 1-ethyl-7-(5*H*-1,2,3,4-tetrahydrocarbazol-5-yl)-6-fluoro-4-oxo-1,4-dihydroquinoline-3-carboxylate (**FQB-1**). **B)** Difluoroboranyl 1-ethyl-7-(1*H*-benzimidazol-1-yl)-6-fluoro-4-oxo-1,4-dihydroquinoline-3-carboxylate (**FQB-2**). **C)** Difluoroboranyl 1-ethyl-6-fluoro-4-oxo-7-(uracil-1-yl)-1,4-dihydroquinoline-3-carboxylate (**FQB-3**). **D)** Difluoroboranyl 1-ethyl-7-(5,5-diphenylhydantoin-3-yl)-6-fluoro-4-oxo-1,4-dihydroquinoline-3-carboxylate (**FQB-4**). **E)** Difluoroboranyl 1-ethyl-7-(3,5-diethoxycarbonyl-2,6-dimethyl-1,4-dihydropyridin-1-yl)-6-fluoro-4-oxo-1,4-dihydroquinoline-3-carboxylate (**FQB-5**). **F)** 1-ethyl-7-(5*H*-1,2,3,4-tetrahydrocarbazole-5-yl)-6-fluoro-4-oxo-1,4-dihydroquinoline-3-carboxylic acid (**FQH-1**). **G)** 1-ethyl-7-(1*H*-benzimidazole-1-yl)-6-fluoro-4-oxo-1,4-dihydroquinoline-3-carboxylic acid (**FQH-1**). **H)** 1-ethyl-6-fluoro-4-oxo-7-(uracil-1-yl)-1,4-dihydroquinoline-3-carboxylic acid (**FQH-3**). **I)** 1-ethyl-6-fluoro-7-(5,5-diphenylhydantoin-3-yl)-4-oxo-1,4-dihydroquinoline-3-carboxylic acid (**FQH-4**). **J)** 1-(3-carboxy-1-ethyl-6-fluoro-4-oxo-1,4-dihydroquinolin-7-yl)-2,6-dimethyl-1,4-dihydropyridine-3,5-dicarboxylic acid (**FQH-5**).

NMR spectra

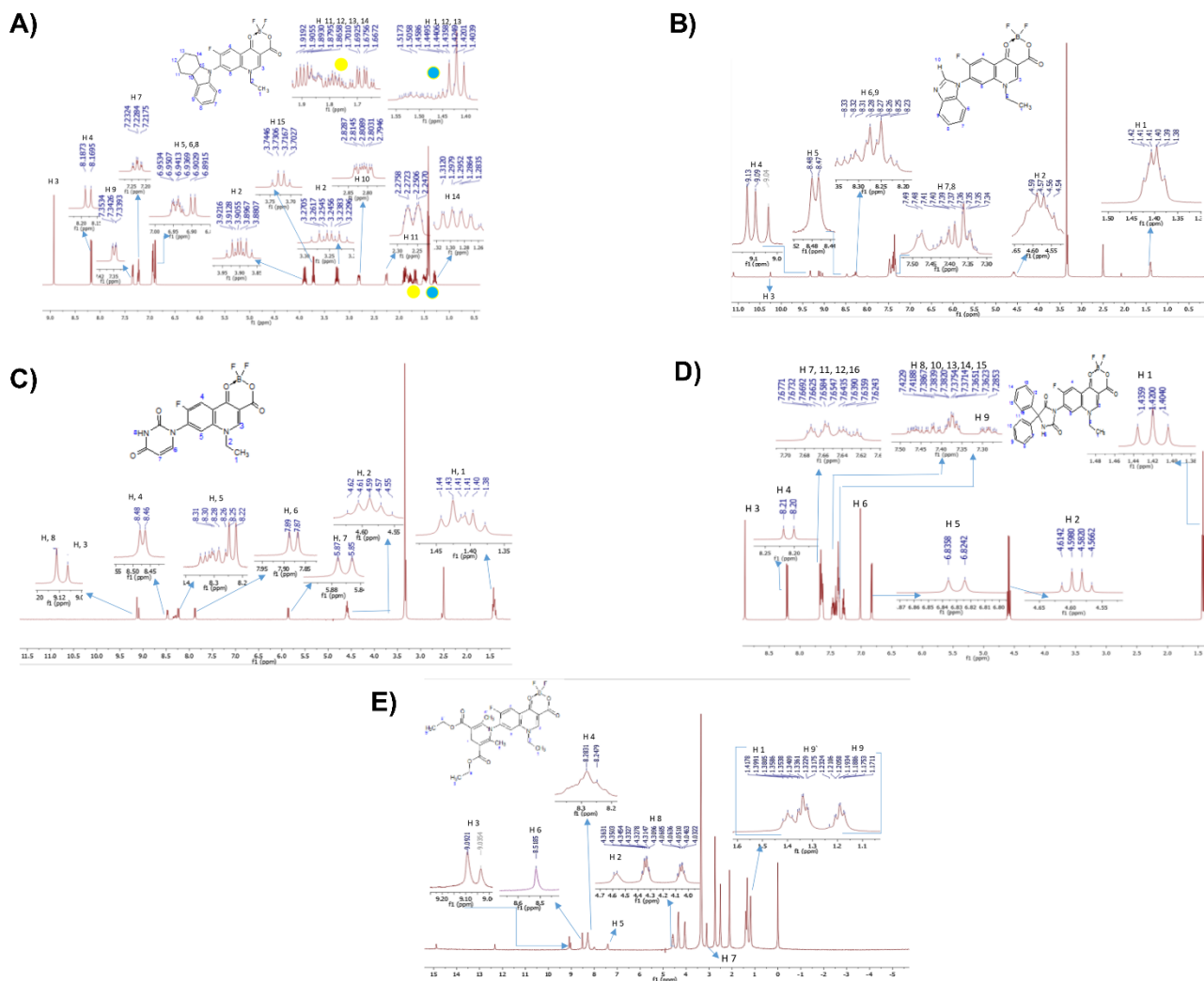


Figure S2. ¹H NMR of fluoroquinolone analogues FQB 1-5. A) Difluoroboranyl 1-ethyl-7-(5*H*-1,2,3,4-tetrahydrocarbazol-5-yl)-6-fluoro-4-oxo-1,4-difluoroboryl dihydroquinoline-3-carboxylate (**FQB-1**). **B)** Difluoroboranyl 1-ethyl-7-(1*H*-benzimidazol-1-yl)-6-fluoro-4-oxo-1,4-dihydroquinoline-3-carboxylate (**FQB-2**). **C)** Difluoroboranyl 1-ethyl-7-6-fluoro-4-oxo-7-(uracil-1-yl)-1,4-dihydroquinoline-3-carboxylate (**FQB-3**). **D)** Difluoroboranyl 1-ethyl-7-(5,5-diphenylhydantoin-3-yl)-6-fluoro-4-oxo-1,4-dihydroquinoline-3-carboxylate (**FQB-4**). **E)** Difluoroboranyl 1-ethyl-7-(3,5-diethoxycarbonyl-2,6-dimethyl-1,4-dihydropyridin-1-yl)-6-fluoro-4-oxo-1,4-dihydroquinoline-3-carboxylate (**FQB-5**).

Thin Layer Chromatography

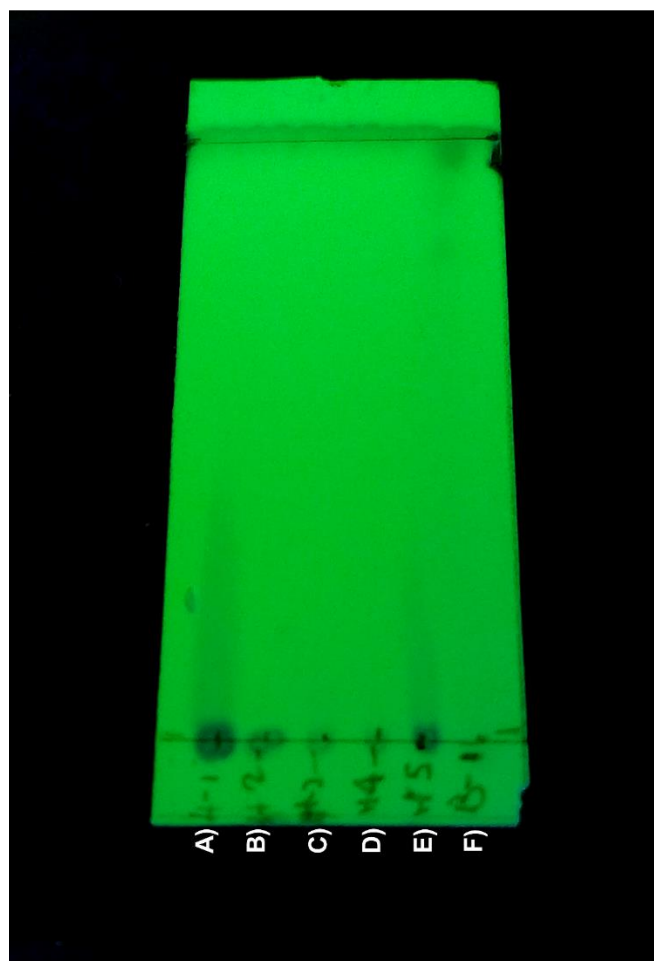


Figure S3. Thin Layer Chromatography (TLC) of fluoroquinolone analogues FQH 1-5. The TLC was made of **A) FQH-1** (7-(2,3,4,5-tetrahydro-carbazol-1-yl), **B) FQH-2** (7-benzimidazol-1-yl), **C) FQH-3** (7-uracil-1-yl), **D) FQH-4** (7-[5,5-diphenyl-hydantoin-1-yl]), **E) FQH-5** (7-[3,5-diethoxycarbonyl-2,6-dimethyl-1,4-dihydropyridin-yl]) and **F) FQB-1** (Difluoroboryl 7-(2,3,4,5-tetrahydro-carbazol-1-yl) in aqueous solution of distilled water and NaOH 0.25N (basic pH), using silica gel plate and a solution of acetonitrile/ethanol (95:5), as mobile phase.